Habitable Planet, 2026, 2(1), 128–148

Scilight

Habitable Planet

Journal Homepage: https://www.sciltp.com/journals/hp

Review

Geothermal Cesium Resources in the Tibetan Plateau: Geological Controls, Resource Potential, and Implications for Low-Carbon Energy Transition

Fei Xue

School of Earth Sciences and Engineering, Hohai University, Nanjing 210098, China; fei.xue@hhu.edu.cn

ABSTRACT

Cesium (Cs) is a strategic metal used in high-precision timing and advanced electronics technologies, but current supply comes mainly from a few pegmatites as associated minerals. This concentration, together with rising demand, creates clear risks for global supply chains. In this context, this study reviews the geological setting, enrichment processes and resource potential of unique geothermal-type Cs resources on the Tibetan Plateau, and its relevance for critical metal security and the energy transition. Hydrochemical, isotopic, petrological and geophysical data show that southern Tibet hosts a distinct geothermal Cs province, where high-temperature systems along Yarlung Zangbo Suture and N–S trending rifts are consistently enriched in Cs in both fluids and siliceous deposits, well above levels in most other geothermal fields worldwide. The evidence supports a crustal evolved magmatic–hydrothermal fluid source model: Himalayan crust undergoes partial melting and magmatic differentiation, releases Cs-rich fluids that rise along fault zones, and the mixed geothermal waters are then trapped in opal-rich siliceous sinters, ancient siliceous rocks and sediment-hosted units. Tibetan geothermal systems therefore contain a dual Cs resource, with both a dissolved flux and a shallow solid inventory in siliceous sinters and sedimentary rocks. Geothermal Cs on the Tibetan Plateau represents a separate geothermal-type deposit, marked by high enrichment, shallow occurrence and close coupling to geothermal heat. Its dispersed, small- to medium-scale nature makes it best suited to co-production with geothermal development. It can enhance the diversity and resilience of Cs supply, while supporting integrated strategies for low-carbon energy deployment and critical metal security.

ARTICLE INFO

History:

Received: 30 November 2025
Revised: 26 December 2025
Accepted: 04 January 2026
Published: 13 January 2026

Keywords:

Cesium mineralization;
Geothermal systems;
Critical mineral resources;
Geothermal–metal co-production;
Tibetan Plateau

Citation:

Xue, F. Geothermal Cesium Resources in the Tibetan Plateau: Geological Controls, Resource Potential, and Implications for Low-Carbon Energy Transition. *Habitable Planet* **2026**, *2*(1), 128–148. https://doi.org/10.63335/j.hp.2026.0030

Research Highlights

- Global cesium supply remains narrow, relying on few pegmatite suites and facing rising strategic demand.
- High-temperature geothermal systems in the Tibetan Plateau host unusually cesium-rich waters and siliceous deposits.
- Multiple lines of evidence support a deep crustal origin, with rare-metal melts feeding upward-moving cesium-bearing fluids.
- Tibetan active springs and shallow siliceous deposits together form substantial cesium resources.
- Shallow geothermal cesium is best developed through distributed co-production with heat and power generation.

1. Introduction

Earth is now facing a marked energy imbalance driven by the rapid growth of fossil-fuel use and population [1, 2]. Rising greenhouse-gas emissions have warmed the climate and intensified extreme events, placing increasing pressure on the long-term habitability of the planet. In response, many countries are pushing for a large-scale shift from fossil fuels to low-carbon and renewable energy sources such as geothermal, wind, solar and hydrogen [3]. This shift, however, rests on secure access to a broad suite of critical mineral resources (CMRs) that underpin clean-energy technologies and advanced electronics [4–6]. Public and policy debates have so far focused mainly on lithium (Li), cobalt (Co) and rare earth elements (REEs), yet alkali metals such as rubidium (Rb) and especially cesium (Cs) are also emerging as strategic metals because of their essential roles in traditional industries and advanced technologies [7, 8].

High grade Cs deposits are concentrated in a handful of hard-rock lithium–cesium–tantalum (LCT) pegmatites and highly fractionated granites (Figure 1), and total identified reserves are only on the order of a few 200,000 t [9–11]. A small number of deposits in a few regions therefore carry a disproportionate share of supply. This strong geographic concentration heightens supply risk and motivates the search for unconventional Cs sources [12]. Some unique geothermal systems have recently attracted attention for this reason. Besides providing low-carbon heat and power, geothermal fluids can be enriched in Li, B, Rb, Cs and other elements, offering the chance for co-producing energy and metals [13–21]. The most successful examples to date are related to Li, with large-scale studies and pilot projects conducted in the Salton Sea (USA) and European geothermal fields for lithium-rich brines, supplemented by detailed studies on resource scale, extraction technologies and environmental performance [16, 19]. Recent studies show that geothermal systems can, under favourable geological conditions, sustain long-term co-extraction of heat and dissolved metals [22]. In contrast, geothermal Cs remains much less explored. Reports of anomalous Cs in hot-spring waters and hydrothermal deposits exist for a few volcanic and continental settings [8, 23–25], but systematic assessments are still rare. This underexploration is somewhat surprising given the fundamental chemical behaviour of cesium. As the largest alkali metal cation, Cs^+ forms highly soluble inorganic compounds and is readily mobilised in aqueous systems through strong hydration, suggesting that geothermal fluids may represent an efficient, yet underappreciated, transport medium for Cs [26].

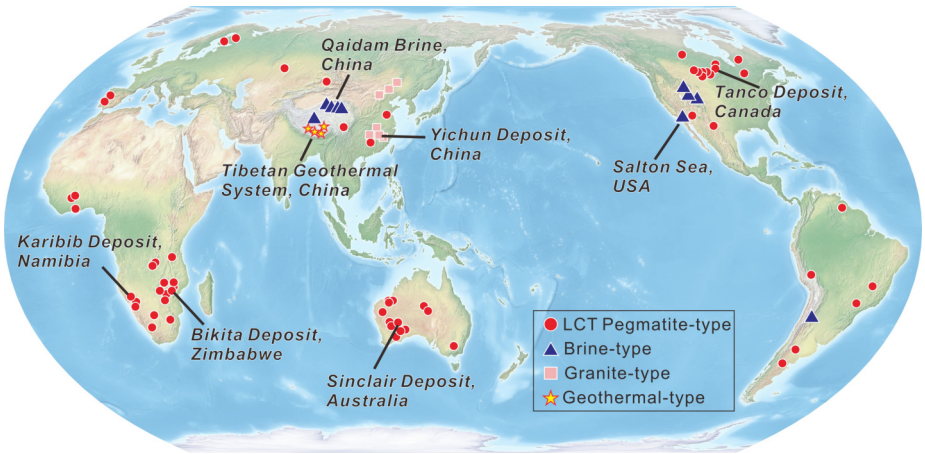

Figure 1. Galobal Distribution of Rb–Cs deposits (modified after [8, 10, 27]). The base global map is from the Equal Earth Physical Map (https://equal-earth.com/physical/) (accessed on 5 November 2025).

As part of the Mediterranean–Himalayan geothermal belt, the Tibetan Plateau (TP) hosts hundreds of hot springs and several high-temperature geothermal fields related to the India–Asia collision and subsequent crustal thickening and extension [25, 28, 29]. Abundant hydrochemical work have shown that many Tibetan systems contain unusually high concentrations of Li, Rb, Cs and B in both spring waters and siliceous sinter, different from geothermal provinces worldwide [8, 21, 23–25, 30–36]. The enrichment of Cs is particularly special: average concentrations in Tibetan spring waters reach several mg/L, with maxima above 70 mg/L, several orders of magnitude higher than typical river water, groundwater and non-orogenic geothermal systems [25].

Our previous work [24, 25] showed that CMR-enriched hot springs in Tibet are systematically aligned with the Yarlung Zangbo Suture and major N–S trending rifts. Elemental and isotopic data point to rare-metal-rich magmatic–hydrothermal fluids derived from partial melting of subducted Indian continental crust as a key source of both heat and metals. Thus, Tibetan geothermal springs act as sensitive "fluid probes" of deep magmatic processes, supply salt lakes [37–41], and may reveal concealed CMR mineralization in the deep. Furthermore, recent work [21] conducted the first systematic estimates of CMR fluxes and reserves in Tibetan geothermal systems and drew attention to a distinctive Cs deposit type: cesium-bearing siliceous sinter developed in Tibetan geothermal fields [42–45]. Detailed work at Chabu further documents the geochemical and isotopic signatures of Cs in sinter [46].

These studies indicate that Tibetan geothermal systems could be regarded as one of the most important non-traditional Cs mineralization provinces globally, with both dissolved and solid-phase resources that may be of strategic interest. However, no systematic review has focused specifically on geothermal Cs in Tibet or elsewhere. Existing studies either discuss Cs with other alkali or critical metals [21, 25] or describe individual siliceous sinter deposits at the local scale [35, 43–45]. As a result, several basic questions are still remaining. How unique are Tibetan Cs concentrations and sinter grades when compared globally? How large is the resource potential in Tibetan spring waters and sinters, and how does it compare with conventional Cs deposits in tonnage, grade and accessibility? Which geological and geochemical processes control the source, migration, enrichment and fixation of Cs? And how might Cs recovery from geothermal systems be integrated into low-carbon development pathways in practice?

This review paper brings together geological, geochemical and resource information to address these gaps and to provide an integrated view of geothermal Cs resources in Tibet. This study outlines the distribution and characteristics of Cs-rich systems, then display Cs abundances in Tibetan geothermal waters and sinters. Then, the controlling factors on Tibetan geothermal Cs's source, enrichment mechanisms are discussed. The Cs resource potentials in both fluids (annual fluxes) and siliceous sinter deposits (reserves) at the regional scale are also evaluated. Finally, the meaning of these resources for the low-carbon energy transition and for long-term Cs supply are considered. By focusing specifically on Cs, this study places Tibetan geothermal systems within the broader context of global Cs geology and highlight their possible role in a more secure and sustainable Cs supply.

2. Global Status of Cesium Resources

2.1. Properties, Applications, and Economic Significance

Cesium is a rare alkali metal (Figure 2) with an average crustal abundance of about 2 ppm [47]. Its large ionic radius (1.67 Å), low ionization potential and strong incompatibility mean that Cs is preferentially concentrated in residual melts and fluids during magmatic differentiation [9, 48]. Discrete Cs-bearing minerals are rare in nature. More often, Cs substitutes for K and Rb in micas and feldspars, or for Na in channel-structured zeolites such as analcime [49]. The main ore mineral is pollucite [48], which forms almost exclusively in highly fractionated LCT pegmatites [9, 10].

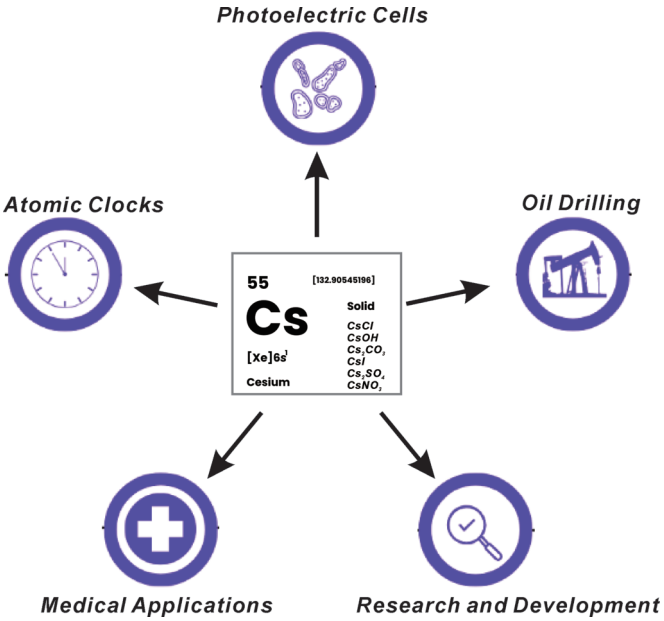

Figure 2. Definition, properties, uses, and major compounds of Cesium. The symbols used in this figure are from Example.com (https://www.examples.com/chemistry/cesium.html) (accessed on 7 November 2025).

Comparatively, global Cs consumption is small, but its physical and chemical properties make it indispensable in several high-value uses (Figure 2). By volume, the largest single application is still cesium formate brine, used as a high-density, low-viscosity drilling and completion fluid in oil and gas wells [50, 51]. Growing strategic interest, however, comes from high-technology sectors. Cesium is a key component of atomic clocks and time-frequency standards

[52], and is also used in magnetohydrodynamic power concepts [53], ion propulsion engines [54] and a range of photoelectric devices [55]. Beyond these, Cs compounds act as promoters in many catalytic processes [56]. Cesium carbonate is widely used in organic synthesis [57], and Cs radioisotopes are used in medical therapy and sterilisation [58]. Recent market analyses indicate that while traditional uses are likely to level off, demand from high-tech and low-carbon applications is expected to rise [8]. Such as in America, the high-tech fields have accounted for 80% of Cs consumption (Figure 3). Comparatively, the global and Chinese Cs consumption is concentrated on the traditional industry indicating a shift in the future (Figure 3).

2.2. Deposit Types and Global Distribution

Cesium occurs in a variety of geological settings, but economically significant resources are concentrated in a few deposit types (Figure 1). On the basis of geological association and formation mechanism, Cs deposits are commonly grouped into four categories: LCT pegmatite-type, granite-hosted rare-metal type, saline-lake brine-type, and geotherma type [8, 10].

LCT pegmatites have been the dominant commercial source. Classic examples include the Tanco mine in Canada and Bikita in Zimbabwe, where large pollucite ore bodies formed during extreme fractionation of peraluminous granitic melts [10, 49]. Granite-hosted systems can contain large in-place resources, but grades are typically lower. In this type of deposit, Cs is dispersed in lithium micas within elevated granitic domes or cupolas, as illustrated by the Yichun district in South China [59]. Saline-lake brines and geothermal systems are attracting attention as newer sources of Cs. In several brine basins, Cs occurs together with Li and other alkalis, although only a few are being considered for recovery due to their very low concentrations. In southern Tibet, active geothermal fields have deposited unusually Cs-rich siliceous sinters, forming a distinct, high-grade deposit type [42].

The geographic distribution of known resources is highly uneven. Most high-grade pollucite is restricted to the Canadian Shield (Manitoba), the Zimbabwe Craton, and parts of Western Australia (Sinclair) and Namibia (Karibib) [11]. China holds substantial Cs resources, but these are mainly in Yichun granite-type mica deposits [59] and in siliceous sinter deposits in Tibet [44], rather than in large, massive pollucite orebodies [8].

2.3. Global Reserves

Estimating global Cs reserves is complicated by limited public reporting and by the fact that Cs is often produced as a by-product of Li mining. USGS data suggest that global reserves, excluding potential resources in China, have long been quoted at around 220,000 t of Cs_2O [11]. Canada accounts for the largest share, mainly at the Tanco pegmatite, which contains more than 120,000 t Cs_2O equivalent [9]. Zimbabwe follows with about 60,000 t Cs_2O linked to the Bikita pegmatite field [10]. Namibia and Australia contribute smaller but still notable amounts, on the order of 30,000 t and 7000 t, respectively [11]. China uses a different classification system. China identified Cs reserves are about 25,000 t Cs_2O, whereas the broader resource base is estimated to exceed 400,000 t Cs_2O [8]. An important addition to the global Cs reserves is the evaluated potential of the Tibetan geothermal belt which will be discussed in the next section. It is worth noting that high-grade and easily processed pollucite ores are being mined, pushing the industry toward lower-grade lepidolite-bearing granites and new extraction approaches for geothermal and brine-hosted Cs [8, 60].

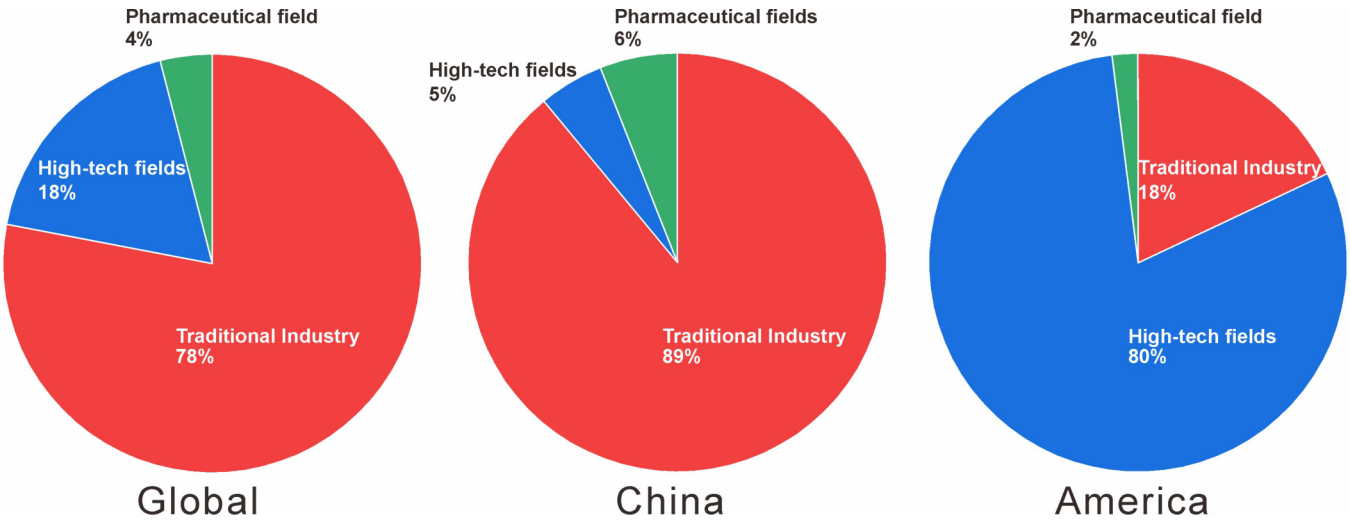

Figure 3. The global, Chinese, and American consumption structures of cesium (modified after [8]).

3. Geological and Geothermal Background of the Tibetan Plateau

The Tibetan Plateau, often referred to as the “Third Pole”, is the highest (average elevation >4500 m) and most extensive (>2.5 million km^2) plateau on Earth [61, 62]. Its formation reflects a long and complex tectonic history. Tectonically, the TP lies between the Himalaya to the south, the Pamir Plateau to the west, the Tarim Craton to the north and the Yangtze Block to the east, forming the world’s largest and highest plateau (Figure 4). The growth of the TP is linked to the evolution of the Tethyan domain from the Proto–Tethys [63], through the Paleo–Tethys [64], to the Neo-Tethys [65], and to the successive collision and accretion of micro-continents along the southern margin of Asia [66]. Closure of the Neo–Tethys Ocean and the onset of the India–Asia collision led to the development of the Banggong–Nujiang Suture and the Yarlung Zangbo Suture, major uplift of the Himalaya and Gangdise Mountains, and ultimately the rise of the TP as a coherent high plateau [61, 66]. Separated by several major sutures and faults, the TP can be divided into five main terranes: the Qaidam Basin, the Songpan–Ganzi terrane, the Qiangtang terrane, the Lhasa terrane and the Himalaya terrane (Figure 4). The Indian plate is still moving northward at a rate of about 50 mm/a. Continued convergence has produced large-scale crustal shortening and underthrusting of Indian lithosphere beneath Tibet, resulting in a markedly thickened crust (locally >60–70 km). At the same time, eastward lateral extrusion and, since the Miocene, widespread east–west extension have generated a series of north–south-trending rifts and grabens across the plateau [28, 67, 68].

Climatically, progressive uplift has led to an extreme continental environment with strong solar radiation, low atmospheric oxygen and pronounced aridity [62]. These conditions favour the development of extensive glaciers, with ice reserves of ~4500 km^3, and the headwaters of many major Asian rivers, including the Yangtze, Yellow, Yarlung Zangbo and Indus. For this reason the TP is often described as the “Asian Water Tower”, with a major influence on regional hydrology and global climate [62, 69]. Intense tectonic activity on the TP is accompanied by widespread magmatism, mineralization and deformation, as well as pronounced geothermal activity. As a key segment of the Mediterranean–Himalayan geothermal belt, the TP hosts abundant geothermal resources, with more than 1700 geothermal springs identified [70]. In the Xizang (Tibet) region alone, over 600–700 geothermal springs and fields have been documented, including boiling springs, hot springs, fumaroles and geysers [71]. Recent work has emphasised the “water–heat–mineral” coupling in these systems, showing that they are important not only for geothermal energy utilisation but also as guides to mineralisation [21, 24, 25, 36]. Their distribution is clearly uneven. Most high-temperature geothermal fields lie within the Lhasa and Himalaya terranes, south of the BNS, whereas the Qiangtang terrane to the north shows weaker activity (Figure 4). Based on spatial distribution and temperature, Tibetan geothermal springs can be grouped into five zones [21, 25] including a low-temperature zone in northern Tibet, a medium- to high-temperature zone in central Tibet, a high-temperature zone in southern Tibet, a medium- to high-temperature zone in western Tibet, and a low- to medium-temperature zone in eastern Tibet (Figure 4). Southern Tibet stands out for its dense and widespread high-temperature geothermal fields, whereas geothermal intensity decreases markedly toward the north–west. This distinctive pattern points to strong tectonic control from deep lithospheric structure, a theme that is central to understanding both geothermal energy resources and associated Cs enrichment on the TP.

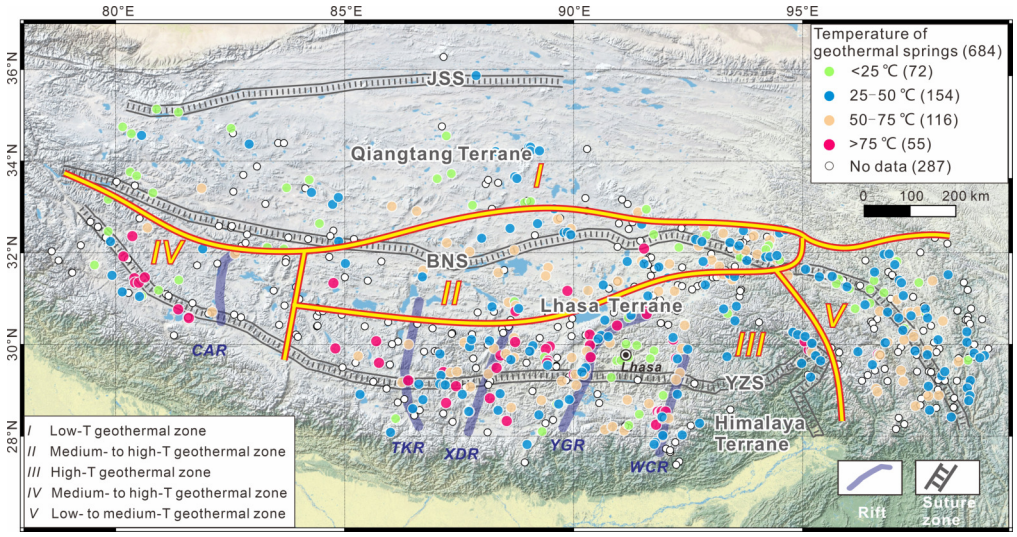

Figure 4. Schematic map of tectonics and distribution of geothermal springs in Tibet. The data of the springs are from [71]. Abbreviations: BNS: Bangonghu–Nujiang Suture; JSS: Jinshajiang Suture; YZS: Yarlung Zangbo Suture; TKR: Tangra Yum Co–Kong Co rifts; CAR: Cuona Co–Aguo Co rifts; WCR: Woka–Cuona rifts; XDR: Xainza–Dinggye rifts; YGR: Yadong–Gulu rifts.

4. Geochemical Characteristics and Distribution of Tibetan Geothermal Cesium

The hydrochemical dataset compiled in *Thermal Springs in Tibet* [71] allows a view of Tibetan geothermal systems. Overall, spring waters have relatively low total dissolved solids (TDS), with a mean of 0.92 g/L well below typical brine thresholds, and neutral or even alkaline water with rarely acid spring water (Figure 5) [31]. In the Piper diagram (Figure 6), most samples plot toward the Na^++K^+ apex of the cation triangle, showing the dominance of alkali cations in Tibetan geothermal waters. Only a small subset shifts toward the Ca^{2+} corner, forming Ca–HCO_3 or mixed Ca–Na–HCO_3 types. In the anion triangle, most points fall along the HCO_3^-+CO_3^{2-}–Cl^- edge, whereas SO_4^{2-}-rich waters are relatively rare. Carbonate–chloride waters are therefore the main hydrochemical type. This overall pattern is similar to many well-studied geothermal systems worldwide (Figure 7). However, geochemical data consistently shows that Tibetan geothermal waters and associated sediments are strongly enriched in several critical elements, especially Cs.

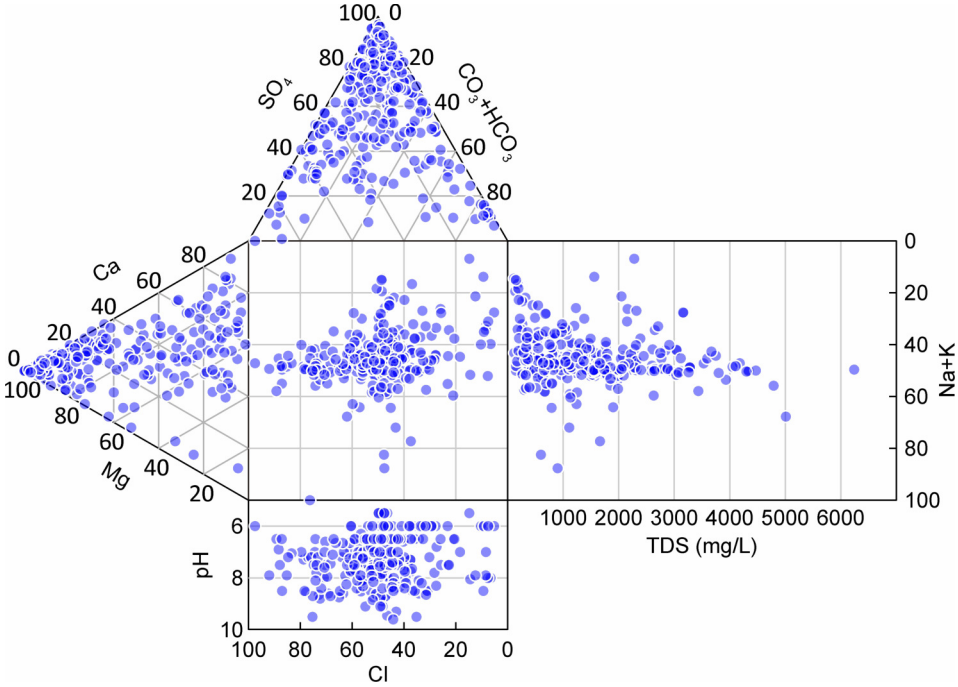

Figure 5. Durov diagram of Tibetan geothermal spring water. The data of the Tibetan spring waters are from [71].

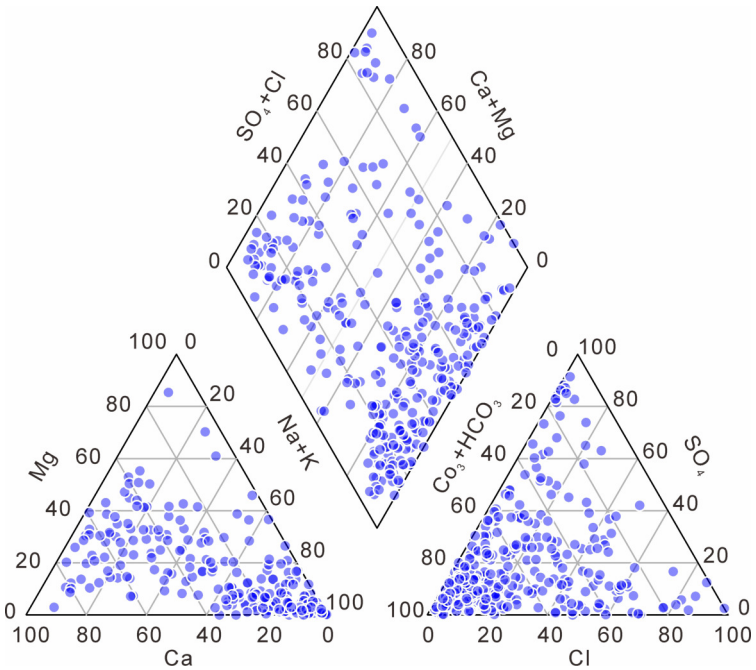

Figure 6. Piper diagram of Tibetan geothermal spring waters. The data of the Tibetan spring waters are from [71].

4.1. Spatial Distribution and Geochemistry of Dissolved Cs in Spring Waters

Dissolved Cs in Tibetan geothermal springs reaches unusually high levels. The average concentration is 3.58 mg/L, several orders of magnitude above typical river water. Comparatively, Cs contents in the upper reaches of major rivers are usually around 0.18–0.22 µg/L [72], and values as low as 0.02 µg/L have been reported for the Rhône River [73]. Across the plateau, 126 springs meet or exceed a commonly used cutoff of 0.5 mg/L Cs, and 6 reach industrial-grade concentration of 20 mg/L [74]. Individual springs can be extreme: Semi contains up to 76.37 mg/L Cs [42], and our work has reported 57.99 mg/L Cs in Zhumaisha [25]. Compared with other geothermal regions, Tibetan springs consistently show much higher Cs contents on a global scale (Figure 7).

Using our previous compilation [25] together with published data, the dissolved Cs concentrations across Tibetan geothermal springs are mapped (Figure 8A). Cs-rich springs are mainly concentrated along the Yarlung Zangbo suture and within N–S trending rifts, with peak enrichment near intersections of these major structures. Important Cs-rich geothermal fields, including Semi, Chatuogang, Gudui, and Zhumaisha all lie in these structurally favourable areas (Figure 8A). From east to west, the main rift zones are Woka–Cuona, Yadong–Gulu, Xainza–Dinggye, Tangra Yum Co–Kong Co and Cuona Co–Aguo Co. These corridors show high geothermal gradients, strong fluid circulation and efficient pathways for deep, metal-bearing fluids to rise and interact with the upper crust. This structural and thermal setting is likely central to the strong Cs enrichment [21, 25, 79]. In addition to Cs, many of the same systems also host elevated Li and Rb (Figure 8B,C), as shown by a growing set of studies from the TP [21, 24, 25, 34, 80, 81]. High-temperature fluids combined with long-lived fracture networks appear to favour multi-element enrichment, a pattern that has only rarely been found in other geothermal systems.

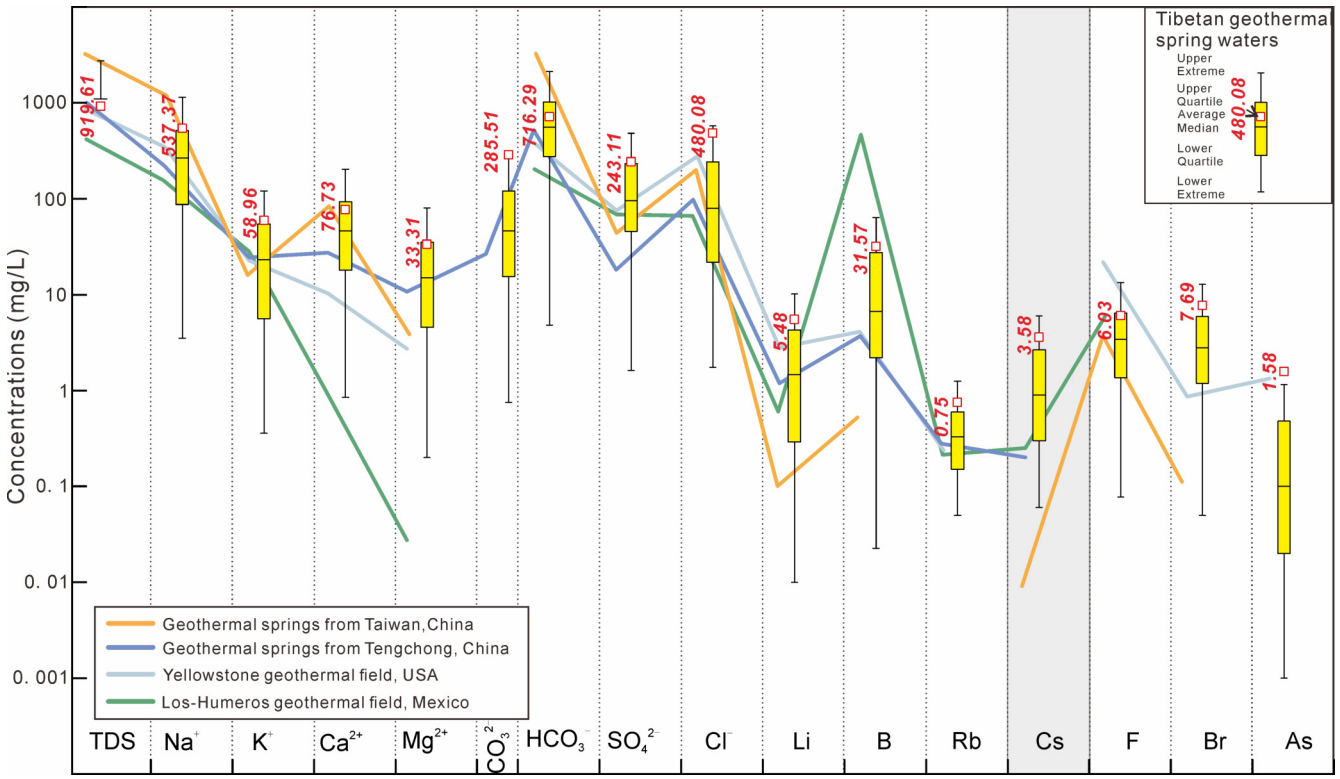

Figure 7. The box pattern of chemical composition of Tibetan geothermal springs. Data for these springs are from [71]. The line chart represents the average water chemical compositions of global geothermal systems. Data source: Tengchong area of China [75], Taiwan Island of China [76], geothermal fields of the Yellowstone National Park in the United States [77], Los Humeros geothermal field in Mexico [78].

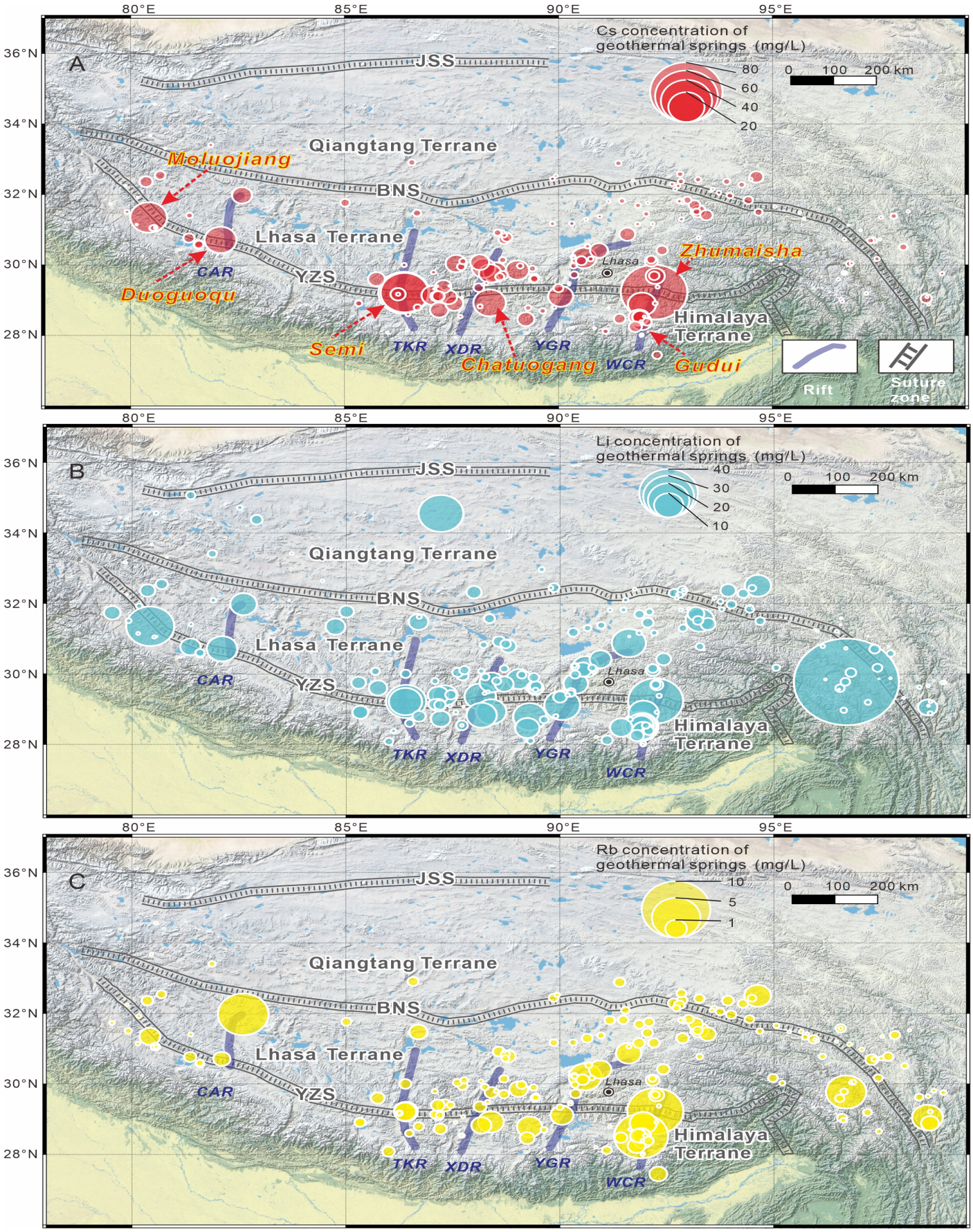

Figure 8. Spatial distribution of Cs (**A**), Li (**B**), and Rb (**C**) in the Tibetan geothermal springs. The data of the springs are from [71]. Abbreviations are same as in Figure 4.

Among these, the Woka–Cuona rift zone is a key area. It is one of the most active geothermal corridors on the TP and includes major fields such as Gudui [82], and Zhumaisha [79]. These fields are marked by high heat flow, vigorous hydrothermal circulation and repeated magmatic–hydrothermal pulses, all of which favour long-term accumulation of dissolved metals [83]. In contrast, the Banggong–Nujiang suture zone and the northern Qiangtang terrane show weaker geothermal activity and host relatively few springs with high Cs (Figure 8A). As a result, the spatial pattern of Cs indicates a first-order control by major plate-bounding sutures and active extensional rifts, underlining the key role of regional tectonics and magmatism in creating and sustaining Cs-rich geothermal systems on TP.

4.2. Cs in Geothermal Deposits and Related Rocks

Cs is also strongly concentrated in solid materials linked to geothermal activity. In Tibetan geothermal fields, the main Cs-bearing solids include siliceous sinters, hydrothermal alteration products and host rocks that have undergone intense fluid–rock interaction. Among these, Cs-rich siliceous sinter is the most distinctive and economically important. It represents an unconventional ore type directly related to high-temperature geothermal systems. This deposit type was first identified and studied in the 1990s [42], marking the beginning of studies on geothermal Cs mineralisation in the region. Since then, Cs-rich siliceous sinter has been reported from several geothermal fields (Figure 9). These siliceous sinters are mainly distributed in the high-temperature belt of southern Tibet (Figure 9), again pointing to the importance of active extension and deep fluid circulation for their formation and preservation.

Previous work has reported average Cs contents of 515 ppm in typical Cs-rich siliceous sinters, with maximum Cs_2O contents of 1.25% [42]. This is far above the commonly cited minimum industrial grade for solid Cs deposits (0.05 wt% Cs_2O) [74] and about two orders of magnitude higher than average upper-crust (2 ppm) [47]. Later work has reported various Cs contents include 2333 ppm at Tagejia [35], 1728 ppm in the Chabu field [46], 1078 ppm at Gulu [44], and 1199, 1497 and 1885 ppm at Buxionglanggu, Baburisu and Babudemi, respectively, in the Gudui geothermal field [84]. Our own work has identified additional Cs-rich sinter in the Chatuogang area (unpublished data). These results indicate that Tibetan siliceous sinters form a coherent, regionally developed Cs mineralisation system, not just a set of isolated anomalies.

Evidence for Cs enrichment also extends beyond modern sinter. In the Gudui field, Jurassic siliceous rocks also show elevated Cs contents, averaging 384 ppm which is close to the minimum industrial grade for solid Cs deposits and therefore of genuine resource interest [85]. Petrographic and geochemical comparisons reveal strong similarities between these Jurassic units and present-day Cs-rich siliceous sinters, including similar REE patterns and elemental ratios [85]. These features support the view that the Jurassic siliceous rocks formed as ancient sinter from hydrothermal fluids and were later modified during diagenesis, alteration and weathering. They can be regarded as “fossil” equivalents of modern siliceous sinter, preserving records of earlier geothermal activity and Cs mineralization. These Mesozoic siliceous rocks are widespread in southern Tibet [86]. Their broad distribution and Cs enrichment imply that favourable conditions for hydrothermal silica and Cs deposition have recurred through geological time.

Our recent work has also pointed to a further type of Cs mineralization hosted by sedimentary rocks in the broader surroundings of geothermal systems (unpublished data). These sedimentary units, located within or near thermal aureoles, show clear overprinting by geothermal fluids and consistently high Cs contents. Both Cs grades and spatial patterns are relatively uniform, forming laterally continuous and stable layers. This combination of elevated but homogeneous Cs concentrations and regular geometry points to a newly recognized style of solid Cs deposit which may offer thicker and more voluminous ore bodies than surface sinters. Future work will focus on these Cs-rich sedimentary rocks, including detailed mapping, mineralogical and geochemical characteristics, and geochronology to clarify their origin, scale and metallogenic significance.

In summary, modern siliceous sinters, their ancient siliceous counterparts and emerging sediment-hosted Cs deposits together show that the TP contains not only world-class Cs-rich geothermal waters, but also diverse and substantial solid-phase Cs resources.

5. Cesium Enrichment Mechanisms in Geothermal Systems

5.1. Sources of Cs in Tibetan Geothermal Systems

Geothermal springs on the TP form within a fairly standard hydrological mechanism: meteoric water or glacial melt infiltrates along faults, is heated at depth, and then rises back to the surface [82]. What is different in Tibet is the very high concentrations of Cs and other highly incompatible elements in many springs. For more than fifty years, the origin of Li, Cs and other critical metals in Tibetan geothermal systems has been debated [23, 25, 87, 88]. Because local precipitation and snowmelt contain only trace amounts of these elements, they must be acquired during subsurface circulation.

Water–rock interaction is the first process to consider. The lithology of the aquifer largely controls the major-ion chemistry of geothermal waters, and hot fluids can certainly leach trace elements from reservoir rocks [88, 89]. The close spatial link between Cs-rich springs and Himalayan leucogranites or pegmatites suggests that these rocks contribute to the system and can locally supply Cs during deep circulation [35]. Several lines of evidence, however, point to limits on this mechanism. Cs (and co-enriched Li, Rb) concentrations in TP springs are much

higher than in classic high-temperature systems where water–rock interaction is known to dominate fluid chemistry [77]. Many Cs-rich waters have very low Mg^{2+} and Ca^{2+} and do not show the large positive $\delta^{18}O$ shifts expected from very strong exchange with host rocks, and their H–O isotopes instead trend toward the magmatic water field [25, 83]. Mass-balance estimates lead to the same conclusion that if present-day Cs fluxes were supplied only by leaching average crust, the required rock volumes would be unrealistically large [79]. These points suggest that water–rock interaction mainly redistributes and buffers Cs within the shallow system, rather than generating the extreme enrichments.

Mantle-derived fluids are another possible source. In volcanic geothermal provinces such as Tengchong and Changbaishan, gas and fluid compositions clearly show a mantle signature reflecting degassing of basaltic magma chambers that supply both heat and volatiles [75, 90]. On the TP, however, Quaternary volcanism is limited, and recent He isotopic data indicate that a strong mantle component is largely restricted to part of the Yangbajing–Damxung basin [28]. More importantly, Cs is a highly incompatible large-ion lithophile element that becomes concentrated in evolved felsic melts, not in mantle-derived basalts [91, 92]. A mainly mantle origin for Cs in southern Tibet is therefore unlikely.

In contrast, multiple lines of evidence indicate a crustal magmatic–hydrothermal source. Geophysical surveys beneath southern Tibet reveal extensive high-conductivity, low-velocity zones in the mid–upper crust, widely interpreted as regions of partial melt or crystal mush (Figure 10) [24, 93]. These bodies coincide with major high-temperature geothermal fields and are comparable to melt zones beneath the Salton Sea and Andean geothermal systems, which act as both heat sources and reservoirs of magmatic fluid [94, 95].

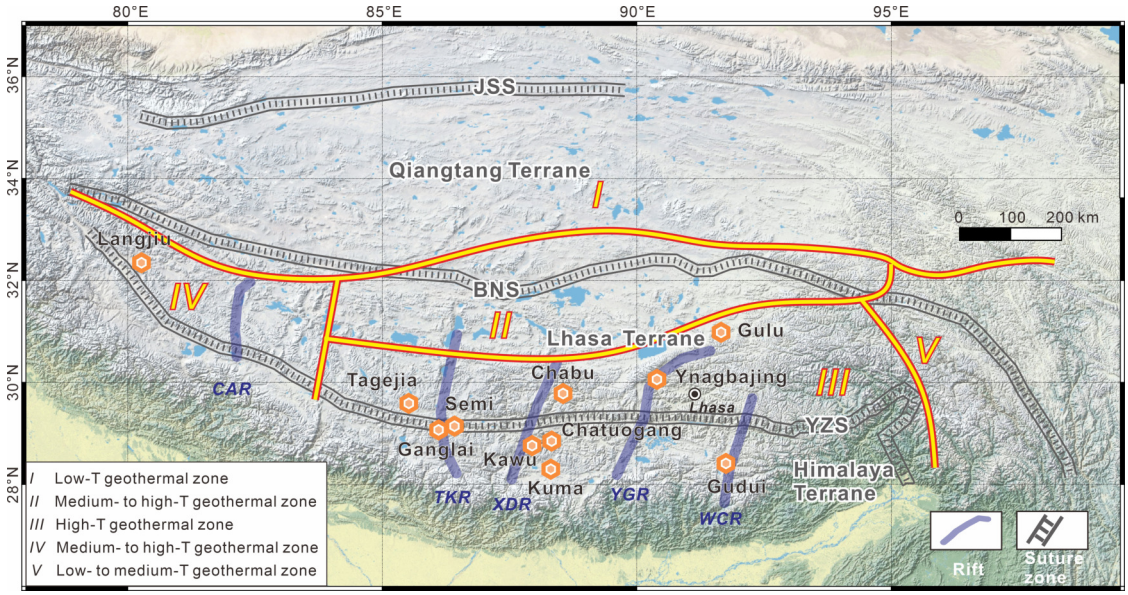

Figure 9. Schematic map showing distribution of Cs rich siliceous sinter in Tibet. Abbreviations are same as in Figure 4.

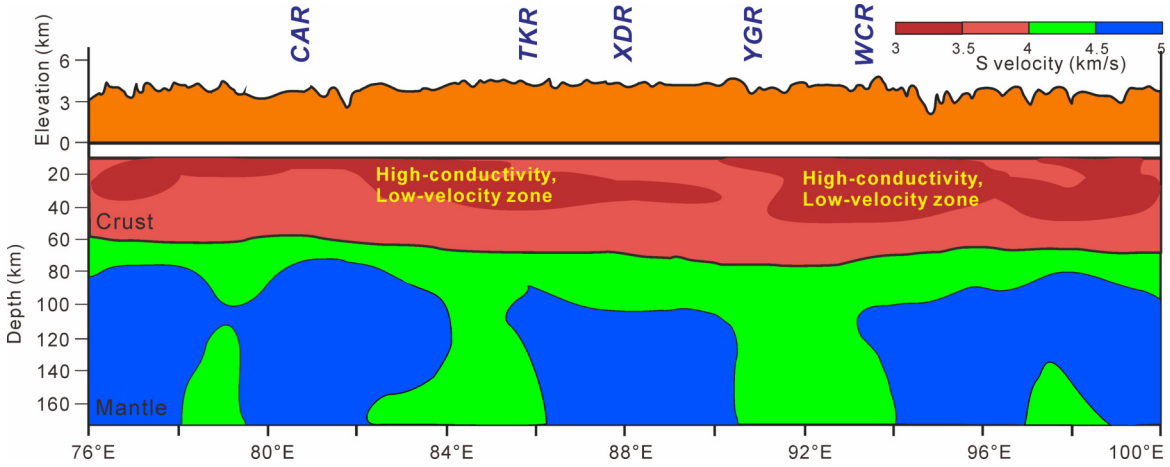

Figure 10. S-velocity cross-section in the southern Tibet showing the distribution of high-conductivity, low-velocity zones in crust (modified after [93]).

Petrological and geochemical data on Himalayan leucogranites and pegmatites provide the evidence. These rocks, abundant in the southern TP crust, contain Li, Rb and especially Cs at well above crustal levels and host several important rare-metal deposits [92, 96, 97]. They are generally interpreted as products of partial melting of rare-metal-enriched Indian continental crust, followed by strong fractional crystallization and late-stage fluid evolution [92]. Thus, Cs is concentrated into the final residual melts and then into exsolved fluids leading to the enrichment of Cs.

The hydrochemistry of Tibetan geothermal waters matches this expectation. Many Cs-rich springs have high B/Cl and Li/Cl ratios and, more importantly, very high Cs/Rb ratios (Figure 11). Natural surface waters and simple rock-leach systems usually show Cs/Rb $\ll 1$ [72, 98], whereas fluids linked to evolved granites and pegmatites can have Cs/Rb$>$1 (Figure 11) [99, 100]. Tibetan hot-spring waters fall into the latter group and define near-linear trends in Cs–Rb space, which can be interpreted as mixing between a Cs-rich magmatic–hydrothermal end-member and dilute meteoric water (Figure 11) [40]. Isotopic tracers support the same conclusion. H–O–B–Li isotopes in Cs-rich springs overlap with those inferred for evolved Himalayan crustal magmas and pegmatites, and waters that plot closer to the magmatic water field tend to have higher Cs contents [25, 101, 102].

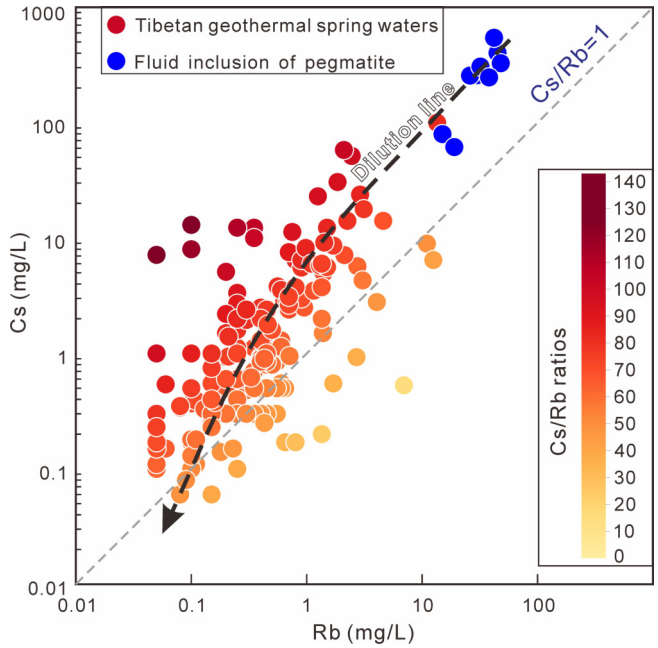

Figure 11. The relationship between Cs and Rb of Tibetan geothermal spring water. The unit of fluid inclusion element content is mg/kg (ppm). The data of Tibetan geothermal spring waters are from [71]. The fluid inclusions of pegmatite are from [100].

Because Cs is more incompatible than Li and is even more strongly concentrated into late magmatic liquids and fluids [100], the observed levels are hard to explain by shallow processes alone. Therefore, the dominant source of Cs in Tibetan geothermal systems is the highly evolved, crust-derived magmatic–hydrothermal fluid released from rare-metal-enriched partial melts in the middle–upper crust.

5.2. Cs Enrichment in Tibetan Geothermal Waters

If crustal partial-melt zones beneath southern Tibet supply Cs-rich magmatic-hydrothermal fluids, then the Cs-rich springs are the result of a multi-stage enrichment process. At the scale of the plateau, the first requirement is the unique geochemical background. National-scale anomaly maps show that southern Tibet, especially the Gangdese belt and the Himalayan region, has some of the strongest Li, Be, Rb and Cs anomalies in China, indicating excellent rare-metal potential [97]. Magmatic rocks in this region including Himalayan leucogranites, pegmatites, intermediate–mafic rocks and adakites, commonly contain Li, Rb and Cs at several to tens of times upper-crust values [97]. For example, Rb and Cs in leucogranites are about 7–8 and 12–13 times higher than average upper crust. This regionally enriched crustal “reservoir” provides the basic chemical precondition for Cs-rich geothermal systems.

Under the background, partial melting is the first step that concentrates Cs into partial melts. In typical silicate systems, Cs behaves as an extremely incompatible element with $K_D^{\text{mineral-melt}} < 0.01$ and an average crustal abundance of only 2 ppm [47]. Once melting starts, Cs is among the first elements to leave the residue and enter the melt. Geochemical modelling of rare-metal pegmatites shows that melts parental to Li–Rb–Cs-rich pegmatites are already enriched in these elements relative to their metasedimentary sources [103]. B-isotope mass-balance calculations for Himalayan leucogranites suggest that Li, Rb and Cs in crust-derived melts can be enriched by roughly a factor of 4–5 during partial melting of metasedimentary rocks [104]. As a result, Cs is efficiently focused into the melt from the outset.

Once generated, these crustal melts rise and pond as magma bodies that evolve through fractional crystallization. As feldspars, micas and other minerals crystallise, more compatible and moderately incompatible elements enter the solids, while Li, Rb and especially Cs remain in the residual melt. With continued differentiation, Cs becomes highly concentrated in a small volume of evolved melt. Studies of granite-related rare-metal systems worldwide identify this differentiation as a key mechanism for concentrating alkali metals and forming LCT pegmatites [9, 92, 96]. The discovery of multiple Li–Be–Cs-bearing deposits and occurrences at Cuonadong, Qiongjiagang, Gabo, Kuqu, Gyirong and elsewhere confirms the strong rare-metal endowment of these evolved magmatic systems [92, 96, 105]. Magmatic differentiation is therefore a second major enrichment step, driving Cs into a small residual melt fraction.

As crystallisation proceeds, the remaining melt becomes progressively richer in H_2O, halogens and other volatiles. Once volatile saturation is reached, a separate aqueous fluid phase exsolves. Experimental and natural

studies show that in such evolved systems Cs is strongly fluid-compatible. During melt–fluid separation, Cs partitions preferentially into the fluid, where its concentration can exceed that in the coexisting melt by several times [106, 107]. Because Cs is the most incompatible and most fluid-loving of the elements considered, the exsolved magmatic–hydrothermal phase can become extremely Cs-rich [108]. At this point, a regionally enriched crustal reservoir has effectively been transformed into a focused deep fluid carrying Cs at concentrations orders of magnitude above background. The structural framework of southern Tibet then provides natural pathways for these fluids to interact with circulating groundwater. Major faults and fracture zones along the YZS and the N–S rifts act as conduits both for downward percolation of meteoric water and for upward flow of magmatic–hydrothermal fluids [24, 25, 79, 83]. Where Cs-rich fluids meet deep groundwater, mixing produces geothermal waters with very high Cs contents.

Deep, high-temperature water–rock interaction in the reservoir adds further complexity but appears secondary in terms of Cs supply. At Yangbajing, boreholes record temperatures of 260 °C at 1500 m and 330 °C at 1850 m, and at Gudui geothermal field, ∼195 °C at 230 m with increasing temperatures at greater depth [109]. Under these near-supercritical conditions, fluid acidity and mineral dissolution capacity are high [110]. Given fluid–rock partition coefficients for Cs generally <0.1, Cs tends to enter the fluid, so deep geothermal waters can further leach Cs from reservoir rocks. B-isotope data from TP systems support some additional rare-metal uptake by such high-temperature interaction [35]. However, as summarized in Section 5.1, this process acts on fluids that are already Cs-rich due to magmatic–hydrothermal input. It boosts Cs concentrations but does not create them.

Overall, Cs enrichment in Tibetan geothermal waters reflects a cascade of processes: regionally enriched crustal sources; partial melting that transfers Cs into melts; magmatic differentiation that concentrates Cs in residual melts; exsolution of a Cs-rich magmatic–hydrothermal fluid; and a final stage of deep water–rock interaction that can further enhance Cs levels. Because Cs is the most incompatible alkali element considered, its extreme surface concentrations are best viewed as the integrated outcome of this multi-stage crustal magmatic–hydrothermal evolution (Figure 12A).

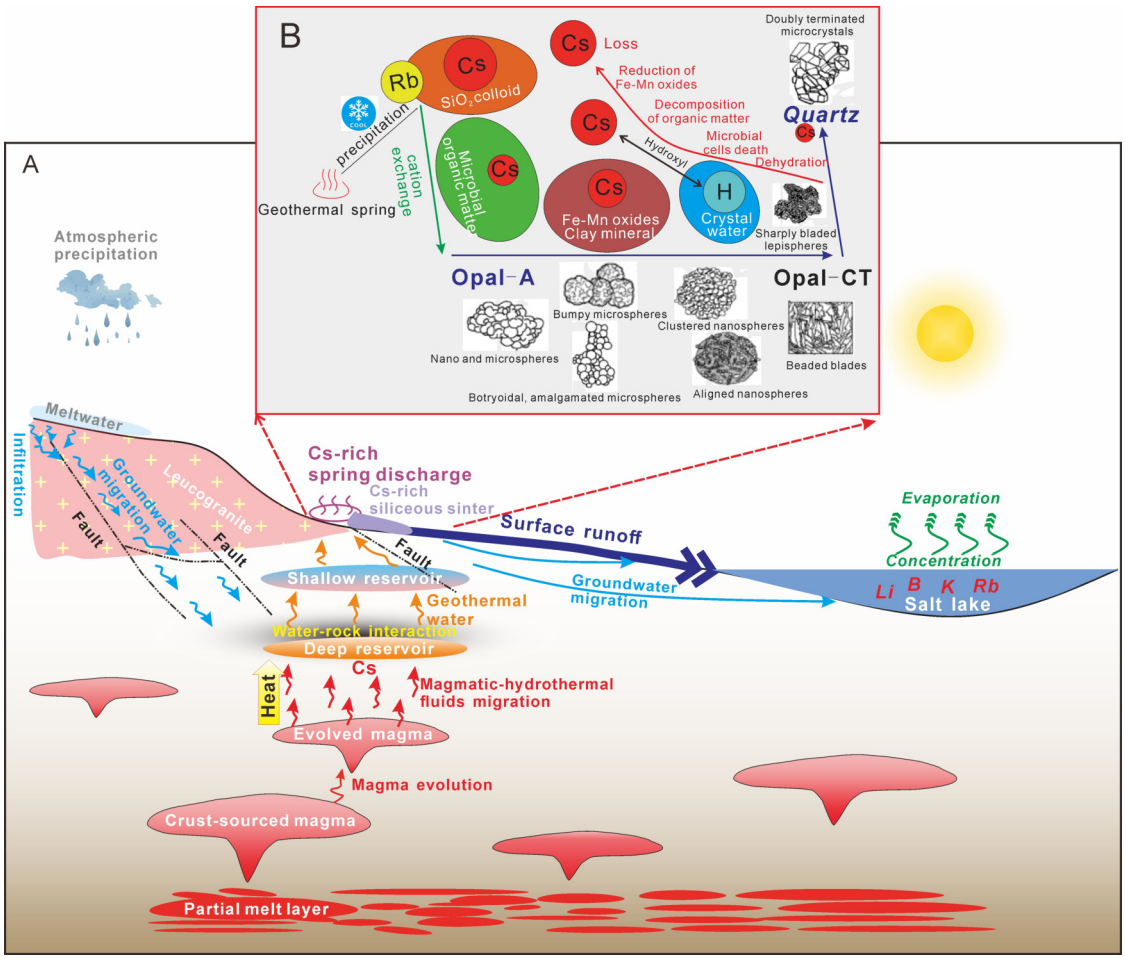

Figure 12. (**A**) Schematic diagram for the enrichment process and resource effects of Cs-riched geothermal spring waters (modified after [25]). (**B**) Conceptual model diagram of mineralisation mechanism of Cs-bearing siliceous sinters (modified after [84]).

5.3. Behaviour and Enrichment of Cs in Siliceous Sinter

Once Cs-rich geothermal waters reach the surface, the focus shifts to near-surface redistribution between fluid and solid phases. In many geothermal regions, siliceous sinter and travertine have been used to reconstruct fluid evolution, trace-element cycling and even hydrothermal microbiology [111–113]. Work from Yellowstone, Taupō, El Tatio and Kamchatka shows that siliceous facies (opal-A/CT, microcrystalline quartz) tend to be the main hosts for trace metals, whereas carbonate travertines usually contain much lower concentrations [31, 114]. Southern Tibet follows the same general pattern, but at far higher Cs levels.

New work in the Gudui field [84] clarifies the enrichment mechanism in sinter. At Gudui and nearby systems, sinter can be grouped into: (1) opal-rich geyserites; (2) mixed silica–carbonate deposits; and (3) calcitic travertine. Cs is overwhelmingly concentrated in opal-rich geyserite, reaching wt%-level Cs_2O in some samples, is moderate in silica–carbonate sinter, and is only at background levels in travertine. This hierarchy is consistent with global observations that amorphous and poorly ordered silica is an efficient sink for many incompatible elements [84, 85, 114], but the magnitude of Cs enrichment in Tibetan siliceous sinters is exceptional.

Element-partitioning behaviour helps explain this pattern. Data from southern Tibet show that Li, B, Rb and Cs respond very differently once silica starts to precipitate. During discharge and sinter growth, Li stays mainly in solution, whereas Cs and Rb are efficiently removed from the fluid and fixed in the solid [35, 115]. Calculated solid–liquid partition coefficients are highest for Cs [84], in line with experiments on alkali sorption: Cs^+, as the largest and least strongly hydrated cation, is preferentially adsorbed by mineral surfaces and gels [116].

Within siliceous sinter, mineral maturity adds a further control. Studies of non-Cs-bearing systems show that opal-A and opal-CT gradually dehydrate and recrystallize to quartz, accompanied by compaction and loss of pore water [117]. At Gudui, Cs is highest in opal-A/CT geyserites and declines as quartz becomes dominant, though it remains above crustal background [84]. Li often increases toward quartz-rich facies, while Rb tends to peak at intermediate stages. These contrasting behaviors underline the strong association of Cs with young, amorphous silica and suggest that part of the Cs inventory is lost during opal–quartz diagenesis. Other phases within sinter also host Cs. Phase-selective extraction studies in New Zealand, Yellowstone and Tibet highlight the roles of Fe–Mn oxides and silicate lattices as trace-element hosts [114, 115]. At Gudui, Cs in opal-rich geyserites is split between a relatively stable silicate-bound component and a more labile pool associated with Fe–Mn oxides and, to a lesser degree, organic matter [84]. In mixed silica–carbonate sinters, a larger share of Cs is tied to easily reducible and mildly acid-soluble phases, reflecting a greater contribution from clays and fresh Fe–Mn coatings. In travertine, Cs is scarce and largely confined to minor detrital silicates. Combined with textural and spectroscopic data, these results point to several coexisting Cs hosts: amorphous SiO_2 gels, Fe–Mn oxyhydroxides, clay-mineral surfaces and structurally bound sites linked to water of crystallisation in opal [42, 84, 118].

The enrichment mechanism inferred from Gudui is broadly consistent with insights from other geothermal provinces. Large, weakly hydrated cations such as Cs^+ destabilise silica colloids and promote flocculation, favouring co-precipitation of Cs with amorphous SiO_2 near vents [42]. Clay minerals and Fe–Mn oxides, which are abundant in sinter aprons, provide high-affinity sorption sites and further immobilise Cs along flow paths [116, 119, 120]. Microbial mats and biofilms can nucleate silica and Fe–Mn oxides and supply functional groups that can temporarily bind metals [121]. Experimental and field work in Tibetan hot springs suggests that thermophilic microorganisms can accumulate Cs and locally enhance its fixation in siliceous sinters, although the bulk Cs budget remains dominated by inorganic phases [84].

In summary, findings from global sinter systems provide a framework for understanding Tibetan Cs-rich siliceous sinters. Deep magmatic–hydrothermal processes deliver Cs-rich fluids to the surface, and near-surface silica precipitation, sorption onto clays and Fe–Mn oxides, and partial incorporation into opal transfer this Cs into siliceous sinter, especially proximal, opal-dominated geyserites (Figure 12B).

6. Resource Potential of Geothermal Cesium in Tibet

6.1. Flux of Geothermal Cesium in Tibetan Springs

Estimating the resource potential of geothermal Cs first requires a sense of how much Cs reaches the surface each year. For Tibet, this can be approximated by combining spring discharge with dissolved Cs concentrations, using the large hydrochemical dataset compiled by [71]. Long-term observations at the Gudui geothermal field show that both concentrations and flow rates have been relatively stable over the past ∼50 years [71, 82, 87].

In the available data, 185 springs have both reliable Cs analyses and discharge measurements, and can be used for flux estimate (Figure 13). Within this group, six springs reach or exceed the commonly used industrial threshold for Cs brine deposits (≥20 mg/L). Although few, these vents together release on the order of 23 t Cs per year, reflecting their combination of high grade and moderate to high flow. If the threshold is lowered to 0.5 mg/L, roughly 120 springs qualify. Summed over these, the total Cs output rises to ∼202 t/a. When all 185 usable springs are included, the current best estimate of annual Cs flux from TP geothermal waters is ∼233 t. Cs-rich springs are thus relatively scarce, but the integrated Cs throughput already reaches a few hundred tonnes per year. In terms of annual metal movement, this is comparable to many small–medium hard-rock Cs operations, even though the flux is dispersed among numerous sites. These figures should be regarded as lower bounds. Many

early flow measurements used simple volumetric or float methods, and discharge data are missing or highly uncertain [71, 87]. Most springs were also sampled only once or a few times, so seasonal and interannual variations in both discharge and Cs concentration remain poorly constrained.

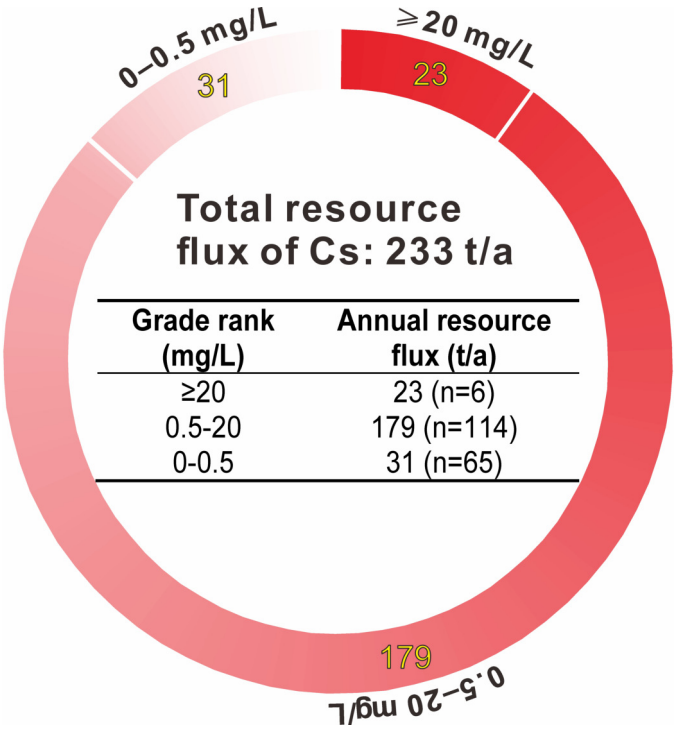

Figure 13. Donut chart of resource flux of Cs in Tibetan geothermal springs.

To improve on this, we have recently re-measured the discharge of nearly 100 representative hot springs across the main Cs-bearing geothermal belts using modern gauging techniques (high-precision current meters, calibrated weirs and, at selected sites, continuous water-level logging). These data provide internally consistent flow estimates that can be coupled directly with updated Cs analyses. For now, the flux values above serve as a conservative baseline. We expect them to be revised upward and better constrained once the new discharge measurements and chemical data are fully integrated.

6.2. Cesium Reserves in Siliceous Sinter and Siliceous Rocks

Where high-temperature fluids discharge at the surface, a considerable share of dissolved Cs is trapped in siliceous sinter building a solid-phase reservoir that complements the dissolved flux. Early work in southern Tibet mapped several Cs-bearing sinter bodies and produced first-order reserve estimates based on exposed area, approximate thickness and average grade (Figure 9) [42].

Three systems stand out in these early calculations.

(1) **Tagejia**. The sinter covers ∼4.19 $\times 10^5$ m^2, with thicknesses of ∼2–15 m. Reported Cs grades range from 0.08 to 0.26 wt%, giving a reserve of 14,459 t Cs when combined with bulk density estimates.

(2) **Gulu.** Exposed Cs-bearing siliceous sinter covers ∼1.01 $\times$ 10^5 m^2 and averages ∼5 m in thickness. Cs contents of 0.05–0.10 wt% corresponds to ∼969 t Cs in place.

(3) **Semi.** Along the steep banks of the Yarlung Zangbo River, siliceous sinter exposures are small (∼1020 m^2) but relatively thick (∼8.3 m) and extremely enriched (up to 1.30 wt% Cs_2O), adding ∼25 t Cs.

Taken together, these three systems contain ∼15,454 t Cs fixed in siliceous sinters [42]. These early estimates were necessarily based on coarse 2D mapping and sparse sampling. To reduce uncertainties in both volume and grade distribution, we have carried out more detailed work in several key targets including Tagejia, Chabu, the Gudui geothermal field (Buxionglanggu, Sagalangga, Riruo, Chaka and Baburisu) and Chatuogang—using UAV-based high-resolution 3D models, handheld XRF, dense sampling and tighter resource modelling. Preliminary results show that once these methods are applied, estimated Cs reserves in several fields increase markedly relative to the original calculations. In particular, the total Cs tonnage in the Gudui, Chabu and Chatuogang sinter complexes each appears to exceed 10,000 t (unpublished data), and the revised reserves for Tagejia is likely higher than the original 14,459 t. Although these upgraded numbers are still being refined and are not reported in detail here, they point to a solid-phase Cs endowment in Tibetan siliceous sinters that is much larger than previously recognised, potentially reaching several $\times$ 10^4 t when all major systems are included. In addition to siliceous sinters, Cs-enriched siliceous rocks and Cs-rich sedimentary units also show significant resource potential. We are currently conducting more detailed mapping and sampling of these lithologies to clarify their origins and better constrain their Cs contents.

In summary, it is obtained that the dissolved Cs resource flux on the order of a few 10^2 t/a, and a solid-phase inventory of at least several $\times$ 10^4 t fixed in siliceous sinter and related rocks, with additional potential in associated siliceous and sedimentary rocks.

7. Development Models and Implications for the Energy Transition

7.1. Characteristics and Development Positioning of Geothermal Cs Resources

The above discussion demonstrates that the Tibetan Cs resources are hosted in a coupled fluid–solid system that offers several possible pathways for utilisation. Compared with conventional pegmatite- and brine-type Cs deposits, geothermal Cs shows a distinct set of features. At First, the main Cs-bearing bodies are very shallowly buried or directly exposed, and can locally reach high grades, especially in proximal opal-A/CT facies [84]. Secondly, individual fields are moderate in size, but occurrences are

highly dispersed. The result is a belt of numerous, small- to medium-scale, structurally aligned "pockets" rather than a few very large ore bodies. Thirdly, the dissolved Cs inventory is tied to active hydrothermal circulation and heat extraction. Cs availability is therefore linked to how geothermal systems operate and evolve, not only to static solid reserves. Thus, geothermal Cs is best seen not as a substitute for large hard-rock deposits, but as a shallow, quasi-renewable supplementary resource that should be developed together with geothermal energy. The most realistic model is to integrate Cs co-recovery from geothermal fluids and nearby siliceous deposits into power generation, district heating and other geothermal projects, using embedded treatment units rather than stand-alone mines.

Such distributed, small- to medium-scale co-production units can raise the overall resource output of individual geothermal projects and add flexibility and resilience to Cs supply in the wider context of the energy transition and critical-metal security. In this sense, geothermal Cs plays a similar role to Li co-production from geothermal brines, which has already been tested at pilot or pre-commercial scale in several fields, for example the Salton Sea in the USA [19, 122], the Upper Rhine Graben [15], and the North German Basin [13, 18]. These projects show that integrating metal recovery with geothermal power and direct-use schemes is technically feasible and can improve project economics, and they provide a useful analogue for future geothermal Cs development (Figure 14). However, it is worthy to note the different features of Li and Cs. Compared with lithium, the co-production of cesium from geothermal fluids faces several distinct technical challenges. Cesium typically occurs at lower concentrations and must be selectively separated from chemically similar alkali ions such as K^+ and Rb^+, placing stringent demands on sorbent selectivity and process control [60]. In addition, while a range of direct lithium extraction technologies have reached pilot or pre-commercial maturity, equivalent large-scale, geothermal-specific technologies for Cs recovery remain less developed and largely confined to ion-exchange or specialty adsorption approaches [123]. These differences imply that Cs co-production will likely be site-specific and best implemented as modular add-ons to geothermal facilities, rather than as standardized, large-throughput extraction systems.

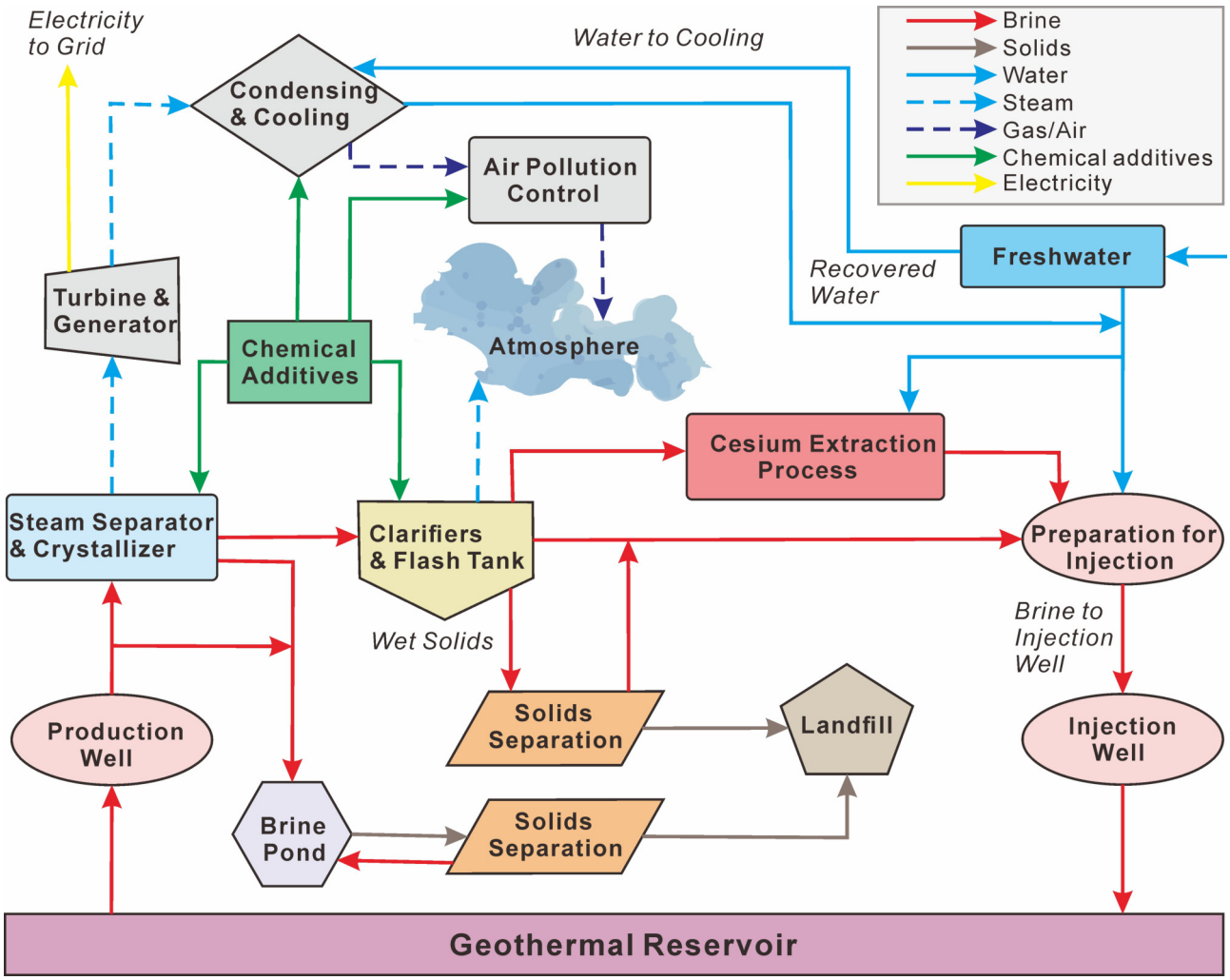

Figure 14. Simplified geothermal process schematic combined with Cs extraction process (modified after [122]).

7.2. Significance of Tibetan Geothermal Cs Resources for China and Global Supply

Forecasts suggest that China's Cs use has entered a sustained growth phase, with demand around the mid-2020s expected to reach ∼1000 t (as Cs_2O), increasingly driven by high-tech and defence applications [8]. Effective domestic supply, however, still comes mainly from a few LCT-pegmatite deposits in Jiangxi, while the economic prospects of large granite-type resources and part of the salt-lake inventory remain uncertain [8, 27]. Internationally, primary Cs output is likewise concentrated in a small number of pegmatite camps such as Tanco and Bikita [10, 11]. Growing demand combined with highly concentrated supply creates a structurally tight and risk-prone market.

This study support defining the Cs associated with geothermal activity on the Qinghai–Tibet Plateau as a separate, geothermal-type Cs resource. Although its total endowment is probably modest compared with the largest pegmatite provinces, this belt adds a new deposit type and a new metallogenic domain to China's Cs portfolio, with direct implications for national and global critical-metal supply.

For China, several points stand out: (1) **Greater geological and spatial diversity**. Geothermal Cs increases both the geological styles and the geographic spread of the domestic Cs base. Even partial utilisation can reduce reliance on a single ore type and one main mining region, and help buffer risks linked to delays or failures in bringing granite-type projects into production [8, 27]. (2) **Alternative exploration and development paths**. The shallow, structurally controlled nature of these systems calls for a different exploration strategy and development model from classic pegmatites. It favours staged, distributed projects that can be integrated with regional development plans on the Plateau. (3) **Stronger position in the global supply chain**. Demonstrating that China controls not only conventional pegmatites and overseas equity, but also a distinct geothermal Cs province, strengthens its position in future negotiations along the global Cs supply chain [21, 25].

At the global scale, recognition of Tibetan geothermal Cs broadens the conceptual space for Cs and Rb–Cs deposits beyond classical LCT pegmatites and salt-lake brines [11]. Because other high-enthalpy geothermal belts exist in tectonically active regions worldwide, the TP examples provide an exploration analogue and methodological reference for targeting Cs (and potentially other critical metals) in geothermal settings elsewhere. In the longer term, if geothermal Cs resources can be delineated and brought into production in more than one region, they could contribute to a more diversified and resilient global Cs supply network.

As a result, geothermal Cs enrichment on the Tibetan Plateau does not replace large conventional Cs mines, but it changes the geometry of both domestic and international supply. By adding a new deposit type, a new metallogenic province and a potential new production domain, it strengthens China's bargaining position in global Cs trade and offers the high-tech sector an additional, geologically distinct source of this critical metal.

7.3. Implications of Geothermal Cs Development for the Energy Transition

From an energy-transition perspective, the main value of Tibetan geothermal Cs lies in coupling firm low-carbon energy with critical metals. As discussed above, Cs in Tibetan geothermal systems is hosted in shallow siliceous deposits and in circulating fluids, and is most realistically recovered through co-production with geothermal power or heat. Each step in expanding geothermal use on the Plateau can simultaneously help decarbonise the energy system and stabilise Cs supply [8, 20]. In the aspect of the energy use, geothermal resources provide stable, dispatchable output that can complement variable wind and solar, improving system reliability and reducing total system costs in high-renewable power systems [124, 125]. Many studies emphasise that flexible geothermal operation can lower the need for storage and backup fossil capacity, and can also supply low-carbon industrial and district heat [126–128]. Embedding Cs extraction units into such projects does not change the thermodynamic role of the plant, but adds an extra revenue stream. Techno-economic assessments for Li show that mineral co-production from geothermal brines can significantly improve project economics and expand the range of commercially viable reservoirs [13, 18], providing a strong analogue for Cs.

At the same time, global studies warn that constraints on critical minerals could slow low-carbon technology deployment and push up costs if supply is not diversified in time [129, 130]. In China, rapid growth in high-tech and defence-related uses is pushing Cs demand onto a higher trajectory [8]. Tibetan geothermal Cs offers a resource option that is geologically and spatially independent from Jiangxi pegmatites and salt-lake systems, and that can lessen reliance on a small number of overseas LCT pegmatite operations. Its absolute scale is likely moderate, but its modular and adjustable production profile means it can act as a flexible buffer within the wider Cs supply portfolio [21].

Relative to new large open-pit or underground mines, adding metal recovery to existing or planned geothermal facilities also has environmental advantages. Life-cycle and techno-economic studies for geothermal Li recovery point to substantially lower greenhouse-gas emissions, land use and, in some cases, water consumption than conventional brine or hard-rock routes, especially when heat and wells are shared and brine is reinjected [17, 131]. While separation technologies for Cs differ from those for Li, the basic system characteristics are similar (Figure 14) [20]. For the ecologically sensitive TP, obtaining part of the required Cs through such development model, rather than through entirely new mines, is important for balancing resource use with strict environmental and ecological constraints.

Policy goals provide an additional layer of motivation. China's "dual-carbon" targets and the associated "1+N" policy framework emphasise both raising the share of non-fossil energy and safeguarding key mineral supplies [132]. Thus, Tibetan geothermal Cs can support the build-out of western clean-energy bases while providing a traceable, relatively low-carbon domestic Cs source for strategic industries. If engineering and regulatory experience from geothermal Li projects can be adapted to Cs, the Tibetan geothermal belts may evolve into demonstration zones where low-carbon energy and critical metals are co-produced in an integrated way, improving project economics and giving China another tool to coordinate energy transition, resource security and regional development.

8. Conclusions and Future Research Directions

8.1. Main Conclusions

(1) Globally, Cs supply still comes mainly from a few LCT pegmatite camps. As demand from high-tech and defence uses keeps rising, this narrow supply base makes the market fragile.

(2) The Tibetan Plateau hosts a separate geothermal Cs province. High-temperature systems along the YZS and N–S rifts contain very Cs-rich waters and Cs-bearing siliceous deposits, controlled by deep crustal melts and major fault zones.

(3) Geochemical, isotopic and geophysical data point to a crustal magmatic–hydrothermal model. Rare-metal-rich crust melts and differentiates, releasing Cs-rich fluids that move upward along sutures and rifts, and these fluids are then efficiently trapped near the surface in opal-rich geyserites and related rocks.

(4) Taken across the Plateau, geothermal springs release a significant ongoing Cs flux, while siliceous sinters, old siliceous rocks and sediment-hosted units together store a large solid Cs inventory. This defines a dual resource made up of moving fluids and relatively static shallow rocks.

(5) Because it is shallow, moderate in scale and closely tied to geothermal heat, Tibetan geothermal Cs is best used through dispersed co-production with geothermal power and heat, rather than stand-alone mining. In this way it can provide China and the world with an extra, lower-carbon Cs source that adds security without replacing large hard-rock mines.

8.2. Future Research Directions

(1) On the geological and genetic side, deeper work is needed in key geothermal corridors. Integrated studies of structure, heat flow and fluid pathways, supported by drilling and systematic sampling, will help refine constraints on Cs sources, fluid evolution and trapping mechanisms. Improved three-dimensional imaging of reservoirs and siliceous bodies is essential for better resource estimates and for resolving how Cs enrichment is organised in space and time.

(2) The wider applicability of the proposed genetic model remains to be tested. Assessing geothermal systems in other active tectonic belts for similar combinations of evolved crustal melts, deeply rooted fault systems and high-enthalpy circulation—such as in the Andes or the Altiplano–Puna region—will help evaluate the model's generality and its value as a guide for identifying geothermal-type Cs enrichment elsewhere.

(3) At the process and engineering level, co-production concepts require field testing. Site-specific, Cs-selective extraction schemes should be evaluated alongside operating or pilot-scale geothermal plants to assess recovery efficiency, operational stability and costs under realistic conditions.

(4) Environmental and system-level assessment should proceed in parallel. Comparative life-cycle analyses of geothermal-only projects, geothermal–Cs co-production and conventional mining are needed to quantify differences in carbon emissions, land use, water demand and ecological impacts, and to position geothermal Cs within broader energy and resource strategies.

Funding

This research was funded by the National Natural Science Foundation of China, Grant No. 42402071, and the Natural Science Foundation of Jiangsu Province, Grant No. BK20241537.

Institutional Review Board Statement

Not applicable.

Informed Consent Statement

Not applicable.

Data Availability Statement

No new data were created or analyzed in this study. Data sharing is not applicable to this article.

Conflicts of Interest

The author declares that he has no known competing financial interests or personal relationships that could have appeared to influence the work reported in this paper. The corresponding author Fei Xue is an Editorial Board Member of this Journal and was not involved in the editorial review or the decision to publish this article.

Use of AI and AI-Assisted Technologies

AI tools were used for polishing the language after which the author carefully reviewed the manuscript and takes full responsibility of the content.

References

1. Santosh, M.; Groves, D.I.; Yang, C.-X. Habitable planet to sustainable civilization: Global climate change with related clean energy transition reliant on declining critical metal resources. *Gondwana Res.* **2024**, *130*, 220–233. https://doi.org/10.1016/j.gr.2024.01.013
2. Shang, Y.; Sang, S.; Tiwari, A.K.; et al. Impacts of renewable energy on climate risk: A global perspective for energy transition in a climate adaptation framework. *Appl. Energy* **2024**, *362*, 122994. https://doi.org/10.1016/j.apenergy.2024.122994
3. Gielen, D. *Critical Minerals for the Energy Transition*; International Renewable Energy Agency (IRENA): Abu Dhabi, United Arab Emirates, 2021.
4. Mathieux, F.; Ardente, F.; Bobba, S.; et al. *Critical Raw Materials and the Circular Economy*; Publications Office of the European Union: Bruxelles, Belgium, 2017.
5. Gulley, A.L.; Nassar, N.T.; Xun, S.; et al. China, the United States, and competition for resources that enable emerging technologies. *Proc. Natl. Acad. Sci. USA* **2018**, *115*, 4111–4115. https://doi.org/10.1073/pnas.1717152115
6. Müller, D.; Groves, D.I.; Santosh, M.; et al. Critical metals: Their applications with emphasis on the clean energy transition. *Geosyst. Geoenviron.* **2025**, *4*, 100310. https://doi.org/10.1016/j.geogeo.2024.100310
7. Varala, R.; Rao, K.S. Cesium salts in organic synthesis: A review. *Curr. Org. Chem.* **2015**, *19*, 1242–1274. https://doi.org/10.2174/1385272819666150507220755
8. Gao, X.R.; Jia, H.X.; Li, T.J.; et al. Perspective of rubidium and caesium resource demand in China. *Acta Geosci. Sin.* **2023**, *44*, 279–285. https://doi.org/10.1111/1755-6724.14302
9. Stilling, A.; Ćerný, P.; Vanstone, P.J. The Tanco Pegmatite at Bernic Lake, Manitoba. XVI. Zonal and bulk compositions and their petrogenetic significance. *Can. Mineral.* **2006**, *44*, 599–623. https://doi.org/10.2113/gscanmin.44.3.599
10. Bradley, D.; McCauley, A.D.; Stillings, L.L. *Mineral-Deposit Model for Lithium-Cesium-Tantalum Pegmatites*; U.S. Geological Survey: Reston, VA, USA, 2017. https://doi.org/10.3133/sir20105070O
11. U.S. Geological Survey. *Mineral Commodity Summaries 2025*; U.S. Geological Survey: Reston, VA, USA, 2025. https://doi.org/10.3133/mcs2025
12. Mudd, G.M.; Jowitt, S.M. Global resource assessments of primary metals: An optimistic reality check. *Nat. Resour. Res.* **2018**, *27*, 229–240. https://doi.org/10.1007/s11053-017-9349-0
13. Alms, K.; Jagert, F.; Blömer, J.; et al. Co-production of geothermal energy and lithium from geothermal waters. In Proceedings of the European Congress, Berlin, Germany, 17–21 October 2022; European Geothermal Energy Council (EGEC): Brussels, Belgium, 2022.
14. Goldberg, V.; Dashti, A.; Egert, R.; et al. Challenges and opportunities for lithium extraction from geothermal systems in Germany—Part 3: The return of the extraction brine. *Energies* **2023**, *16*, 5899. https://doi.org/10.3390/en16165899
15. Koelbel, L.; Kölbel, T.; Herrmann, L.; et al. Lithium extraction from geothermal brines in the Upper Rhine Graben: A case study of potential and current state of the art. *Hydrometallurgy* **2023**, *221*, 106131. https://doi.org/10.1016/j.hydromet.2023.106131
16. Sanjuan, B.; Gourcerol, B.; Millot, R.; et al. Lithium-rich geothermal brines in Europe: An up-date about geochemical characteristics and implications for potential Li resources. *Geothermics* **2022**, *101*, 102385. https://doi.org/10.1016/j.geothermics.2022.102385
17. Schenker, V.; Oberschelp, C.; Pfister, S. Regionalized life cycle assessment of present and future lithium production for Li-ion batteries. *Resour. Conserv. Recycl.* **2022**, *187*, 106611. https://doi.org/10.1016/j.resconrec.2022.106611
18. Weinand, J.M.; Vandenberg, G.; Risch, S.; et al. Low-carbon lithium extraction makes deep geothermal plants cost-competitive in future energy systems. *Adv. Appl. Energy* **2023**, *11*, 100148. https://doi.org/10.1016/j.adapen.2023.100148
19. Busse, M.M.; McKibben, M.A.; Stringfellow, W.; et al. Impact of geothermal expansion and lithium extraction in the Salton Sea known geothermal resource area (SS-KGRA) on local water resources. *Environ. Res. Lett.* **2024**, *19*, 104011. https://doi.org/10.1088/1748-9326/ad6a73
20. Subasinghe, H.C.S.; Zhang, H.; Shi, F.; et al. Critical minerals extraction from geothermal brines. *Joule* **2025**, *9*, 102171. https://doi.org/10.1016/j.joule.2025.102171
21. Wang, D.; Xue, F.; Ren, L.; et al. Critical minerals in Tibetan geothermal systems: Their distribution, flux, reserves, and resource effects. *Minerals* **2025**, *15*, 93. https://doi.org/10.3390/min15010093
22. Banshoya, S.I.; Berre, I.; Keilegavlen, E. A simulation study of the impact of fracture networks on the co-production of geothermal energy and lithium. *Geotherm. Energy* **2025**, *13*, 31. https://doi.org/10.1186/s40517-025-00356-3
23. Grimaud, D.; Huang, S.; Michard, G.; et al. Chemical study of geothermal waters of Central Tibet (China). *Geothermics* **1985**, *14*, 35–48. https://doi.org/10.1016/0375-6505(85)90092-6
24. Tan, H.B.; Shi, Z.W.; Cong, P.X.; et al. The spatial distribution law of B, Li, Rb and Cs elements and supernormal enrichment mechanism in Tibet geothermal system. *Sediment. Geol. Tethyan Geol.* **2023**, *43*, 404–415. https://doi.org/10.19826/j.cnki.1009-3850.2023.02001
25. Xue, F.; Tan, H.; Zhang, X.; et al. Sources, enrichment mechanisms, and resource effects of rare metal elements-enriched geothermal springs in Xizang, China. *Sci. China Earth Sci.* **2024**, *67*, 3476–3499. https://doi.org/10.1007/s11430-024-1413-0
26. Greenwood, N.N.; Earnshaw, A. *Chemistry of the Elements*; Elsevier: Oxford, UK, 2012.
27. Sun, Y.; Wang, D.H.; Wang, C.H.; et al. Metallogenic regularity, new prospecting and guide direction of rubidium deposits in China. *Acta Geol. Sin.* **2019**, *93*, 1231–1244. https://doi.org/10.19762/j.cnki.dizhixuebao.2019183
28. Klemperer, S.L.; Zhao, P.; Whyte, C.J.; et al. Limited underthrusting of India below Tibet: $^{3}He/^{4}He$ analysis of thermal springs locates the mantle suture in continental collision. *Proc. Natl. Acad. Sci. USA* **2022**, *119*, e2113877119. https://doi.org/10.1073/pnas.2113877119
29. Tamburello, G.; Chiodini, G.; Ciotoli, G.; et al. Global thermal spring distribution and relationship to endogenous and exogenous factors. *Nat. Commun.* **2022**, *13*, 6378. https://doi.org/10.1038/s41467-022-34115-w
30. Elenga, H.I.; Tan, H.; Su, J.; et al. Origin of the enrichment of B and alkali metal elements in the geothermal water in the Tibetan Plateau: Evidence from B and Sr isotopes. *Geochemistry* **2021**, *81*, 125797. https://doi.org/10.1016/j.chemer.2021.125797
31. Guo, Q.; Nordstrom, D.K.; McCleskey, R.B. Towards understanding the puzzling lack of acid geothermal springs in Tibet (China): Insight from a comparison with Yellowstone (USA) and some active volcanic hydrothermal systems. *J. Volcanol. Geotherm. Res.* **2014**, *288*, 94–104. https://doi.org/10.1016/j.jvolgeores.2014.10.005
32. Tan, H.; Su, J.; Xu, P.; et al. Enrichment mechanism of Li, B and K in the geothermal water and associated deposits from the Kawu area of the Tibetan Plateau: Constraints from geochemical experimental data. *Appl. Geochem.* **2018**, *93*, 60–68. https://doi.org/10.1016/j.apgeochem.2018.04.001
33. Wang, C.; Zheng, M.; Zhang, X.; et al. Geothermal-type lithium resources in southern Xizang, China. *Acta Geol. Sin.* **2021**, *95*, 860–872. https://doi.org/10.1111/1755-6724.14675
34. Li, J.; Wang, X.; Ruan, C.; et al. Enrichment mechanisms of lithium for the geothermal springs in southern Tibet, China. *J. Hydrol.* **2022**, *612*, 128022. https://doi.org/10.1016/j.jhydrol.2022.128022
35. Li, Y.-C.; Wei, H.-Z.; Palmer, M.R.; et al. Boron isotope constraints on the migration and accumulation of rare alkali metals in the

geyserite cesium deposits in southern Tibet. *Ore Geol. Rev.* **2023**, *163*, 105740. https://doi.org/10.1016/j.oregeorev.2023.105740

36. Li, J.; Li, H.; Ruan, C.; et al. Hydrochemical insights into lithium enrichment mechanisms in southern Tibet's geothermal systems. *J. Geochem. Explor.* **2026**, *280*, 107929. https://doi.org/10.1016/j.gexplo.2025.107929
37. Li, Y.-L.; Miao, W.-L.; He, M.-Y.; et al. Origin of lithium-rich salt lakes on the western Kunlun Mountains of the Tibetan Plateau: Evidence from hydrogeochemistry and lithium isotopes. *Ore Geol. Rev.* **2023**, *155*, 105356. https://doi.org/10.1016/j.oregeorev.2023.105356
38. Miao, W.; Zhang, X.; Li, Y.; et al. Lithium and strontium isotopic systematics in the Nalenggele River catchment of Qaidam Basin, China: Quantifying contributions to lithium brines and deciphering lithium behavior in hydrological processes. *J. Hydrol.* **2022**, *614*, 128630. https://doi.org/10.1016/j.jhydrol.2022.128630
39. Shi, Z.; Tan, H.; Xue, F.; et al. Hydrochemical evolution and source mechanisms governing the unusual lithium and boron enrichment in salt lakes of northern Tibet. *Geol. Soc. Am. Bull.* **2024**, *136*, 5174–5190. https://doi.org/10.1130/B37516.1
40. Xue, F.; Tan, H.; Zhang, X.; et al. Contrasting sources and enrichment mechanisms in lithium-rich salt lakes: A Li–H–O isotopic and geochemical study from northern Tibetan Plateau. *Geosci. Front.* **2024**, *15*, 101768. https://doi.org/10.1016/j.gsf.2023.101768
41. Xue, F.; Tan, H.; Zhang, X.; et al. Geochemical behavior and migration processes of lithium in the coupled geothermal spring-river-salt lake mineralization system in northern Xizang. *Acta Petrol. Sin.* **2025**, *41*, 968–982. https://doi.org/10.18654/1000-0569/2025.03.16
42. Zheng, M.; Wang, Q.; Duo, J.; et al. *A New Type of Hydrothermal Deposit Cesium-bearing Geyserite in Tibet*; Geological Publishing House: Beijing, China, 1995; pp. 113–172.
43. Zhao, Y.; Nie, F.; Hou, Z.; et al. Geological characteristics and formation age of hot spring cesium deposit in Targejia area, Tibet. *Miner. Depos.* **2006**, *25*, 281–291. https://doi.org/10.3969/j.issn.1001-3458.2006.03.003
44. Zhao, Y.; Fan, X.; Han, J.; et al. Geologic and geochemical features and ore forming process for hot spring cesium deposit of Gulu area, Nagqu region, Tibet, China. *Geol. Bull. China* **2009**, *28*, 933–954. https://doi.org/10.3969/j.issn.1671-2552.2009.07.014
45. Wang, W.; Jiang, S.-Y. The silicon isotopic compositions of silica sinters in Xizang, China: Implications for paleo-geothermal activities since 0.5 Ma B.P. *Appl. Geochem.* **2024**, *169*, 106052. https://doi.org/10.1016/j.apgeochem.2024.106052
46. Yang, Z. Geochemical Characteristics of Geothermal Fluids in Chabu Geothermal Field, Xietongmen County, Tibet. Master Thesis, Tibet University, Lhasa, Tibet, China, 2022. https://doi.org/10.27735/d.cnki.gxzdx.2022.000039
47. Rudnick, R.L.; Gao, S. 3.01 – Composition of the continental crust In *Treatise on Geochemistry*; Holland, H.D., Turekian, K.K., Eds.; Pergamon: Oxford, UK, 2003; pp. 1–64. https://doi.org/10.1016/B0-08-043751-6/03016-4
48. London, D.; Morgan, G.B.; Icenhower, J. Stability and solubility of pollucite in the granite system at 200 MPa H_2O. *Can. Mineral.* **1998**, *36*, 497–510. 10.3749/canmin.er00001
49. Černý, P.; London, D.; Novák, M. Granitic pegmatites as reflections of their sources. *Elements* **2012**, *8*, 289–294. https://doi.org/10.2113/gselements.8.4.289
50. Saasen, A.; Jordal, O.H.; Burkhead, D.; et al. Drilling HT/HP wells using a cesium formate based drilling fluid. In Proceedings of the SPE/IADC Drilling Conference and Exhibition, Dallas, TX, USA, 26–28 February 2002; Society of Petroleum Engineers (SPE): Amsterdam, The Netherlands, 2002; p SPE-74541-MS.
51. Berg, P.C.; Pedersen, E.S.; Lauritsen, Å.; et al. Drilling and completing high-angle wells in high-density, cesium formate brine—The Kvitebjørn experience, 2004–2006. *SPE Drill. Complet.* **2009**, *24*, 15–24. https://doi.org/10.2118/112577-PA
52. Jaduszliwer, B.; Camparo, J. Past, present and future of atomic clocks for GNSS. *GPS Solut.* **2021**, *25*, 27–39. https://doi.org/10.1007/s10291-020-01064-9
53. Murakami, T.; Yamasaki, H. Plasma-fluid behavior of a less divergent disk magnetohydrodynamic generator using helium–cesium. *IEEE Trans. Plasma Sci.* **2004**, *32*, 1752–1759. https://doi.org/10.1109/TPS.2004.832551
54. Wang, Z.; Wang, H.; Li, L.; et al. Combustion and plume-plasma characteristics of cesium-based solid propellant. *Combust. Flame* **2024**, *263*, 113419. https://doi.org/10.1016/j.combustflame.2024.113419
55. Qiao, F.; Ma, X.; Qiu, X.; et al. Enhancing atomic layer deposition—microchannel plate gain with Cs activation in photoelectric devices. *Opt. Eng.* **2025**, *64*, 044102. https://doi.org/10.1117/1.OE.64.4.044102
56. Sun, J.; Cai, Q.; Wan, Y.; et al. Promotional effects of cesium promoter on higher alcohol synthesis from syngas over Cs-promoted Cu/ZnO/Al_2O_3 catalysts. *ACS Catal.* **2016**, *6*, 5771–5785. https://doi.org/10.1021/acscatal.6b01446
57. Varala, R.; Achari, K.M.M.; Hussein, M.; et al. Cesium carbonate (Cs_2CO_3) in organic synthesis: A sexennial update (2018 to date). *Curr. Org. Chem.* **2025**, *29*, 2–18. https://doi.org/10.2174/1385272829666241009100505
58. Melnikov, P.; Zanoni, L.Z. Clinical effects of cesium intake. *Biol. Trace Elem. Res.* **2010**, *135*, 355–363. https://doi.org/10.1007/s12011-009-8509-4
59. Wang, R.C.; Hu, H.; Zhang, A.C.; et al. Pollucite and the cesium-dominant analogue of polylithionite as expressions of extreme Cs enrichment in the Yichun topaz–lepidolite granite, southern China. *Can. Mineral.* **2004**, *42*, 883–896. https://doi.org/10.2113/gscanmin.42.3.883
60. Niu, H.; Yu, M.; Mubula, Y.; et al. Extraction of rubidium and cesium from a variety of resources: A review. *Materials* **2025**, *18*, 3378. https://doi.org/10.3390/ma18143378
61. Yin, A. Cenozoic tectonic evolution of the Himalayan orogen as constrained by along-strike variation of structural geometry, exhumation history, and foreland sedimentation. *Earth-Sci. Rev.* **2006**, *76*, 1–131. https://doi.org/10.1016/j.earscirev.2005.05.004
62. Yao, T.; Bolch, T.; Chen, D.; et al. The imbalance of the Asian water tower. *Nat. Rev. Earth Environ.* **2022**, *3*, 618–632. https://doi.org/10.1038/s43017-022-00299-4
63. Li, S.; Zhao, S.; Liu, X.; et al. Closure of the Proto-Tethys Ocean and early Paleozoic amalgamation of microcontinental blocks in East Asia. *Earth-Sci. Rev.* **2018**, *186*, 37–75. https://doi.org/10.1016/j.earscirev.2017.01.011
64. Ding, L.; Yang, D.; Cai, F.L.; et al. Provenance analysis of the Mesozoic Hoh-Xil-Songpan-Ganzi turbidites in northern Tibet: Implications for the tectonic evolution of the eastern Paleo-Tethys Ocean. *Tectonics* **2013**, *32*, 34–48. https://doi.org/10.1002/tect.20020
65. Zhu, R.; Zhao, P.; Zhao, L. Tectonic evolution and geodynamics of the Neo-Tethys Ocean. *Sci. China Earth Sci.* **2022**, *65*, 1–24. https://doi.org/10.1007/s11430-021-9845-7
66. Hou, Z.; Xu, B.; Zheng, Y.; et al. Mantle flow: The deep mechanism of large-scale growth in Tibetan Plateau. *Chin. Sci. Bull.* **2021**, *66*, 2671–2690. https://doi.org/10.1360/TB-2020-0817
67. Nábělek, J.; Hetényi, G.; Vergne, J.; et al. Underplating in the Himalaya–Tibet collision zone revealed by the Hi-CLIMB experiment. *Science* **2009**, *325*, 1371–1374. https://doi.org/10.1126/science.1167719
68. Bian, S.; Gong, J.; Zuza, A.V.; et al. Along-strike variation in the initiation timing of the north-trending rifts in southern Tibet as revealed from the Yadong-Gulu rift. *Tectonics* **2022**, *41*, e2021TC007091. https://doi.org/10.1029/2021TC007091
69. Tan, H.; Chen, X.; Shi, D.; et al. Base flow in the Yarlungzangbo River, Tibet, maintained by the isotopically-depleted precipitation and groundwater discharge. *Sci. Total Environ.* **2020**, *743*, 143510.

https://doi.org/10.1016/j.scitotenv.2020.143510

70. Liao, Z. *Thermal Springs and Geothermal Energy in the Qinghai-Tibetan Plateau and the Surroundings*; Springer: Cham, Switzerland, 2018.
71. Tong, W.; Liao, Z.J.; Liu, S.B.; et al. *Thermal Springs in Tibet*; Beijing Science and Technology Press: Beijing, China, 2000.
72. Chakrapani, G.J. Major and trace element geochemistry in Upper Ganga River in the Himalayas, India. *Environ. Geol.* **2005**, *48*, 189–201. https://doi.org/10.1007/s00254-005-1287-1
73. Ollivier, P.; Radakovitch, O.; Hamelin, B. Major and trace element partition and fluxes in the Rhône River. *Chem. Geol.* **2011**, *285*, 15–31. https://doi.org/10.1016/j.chemgeo.2011.02.011
74. DZ/T 0203–2002. *People's Republic of China Geological and Mineral Industry Standard: Specifications for Rare Metal Mineral Exploration*; Standards Press of China: Beijing, China, 2002.
75. Guo, Q.; Wang, Y. Geochemistry of hot springs in the Tengchong hydrothermal areas, southwestern China. *J. Volcanol. Geotherm. Res.* **2012**, *215–216*, 61–73. https://doi.org/10.1016/j.jvolgeores.2011.12.003
76. Maity, J.P.; Chen, C.-Y.; Bundschuh, J.; et al. Hydrogeochemical reconnaissance of arsenic cycling and possible environmental risk in hydrothermal systems of Taiwan. *Groundwater Sustain. Dev.* **2017**, *5*, 1–13. https://doi.org/10.1016/j.gsd.2017.03.001
77. Cullen, J.T.; Hurwitz, S.; Barnes, J.D.; et al. The systematics of chlorine, lihium, and boron and δ37Cl, δ7Li, and δ11B in the hydrothermal system of the yellowstone plateau volcanic field. *Geochem. Geophys. Geosyst.* **2021**, *22*, e2020GC009589. https://doi.org/10.1029/2020GC009589
78. Bernard, R.; Taran, Y.; Pennisi, M.; et al. Chloride and boron behavior in fluids of Los Humeros geothermal field (Mexico): A model based on the existence of deep acid brine. *Appl. Geochem.* **2011**, *26*, 2064–2073. https://doi.org/10.1016/j.apgeochem.2011.07.004
79. Cong, P.; Tan, H.; Shi, Z.; et al. Unusual boron isotopic value and hydrochemical characteristics of thermal springs indicating magmatic fluids upwelling along Cuona-Sangri Rift in the Tibet (China). *Geothermics* **2025**, *127*, 103222. https://doi.org/10.1016/j.geothermics.2024.103222
80. Wei, S.; Zhang, W.; Fu, Y.; et al. Distribution characteristics and resource potential evaluation of lithium in geothermal water in China. *Geol. China* **2024**, *51*, 1527–1553. https://doi.org/10.12029/gc20230214001
81. Zhu, H.; Tan, H.; Cong, P.; et al. Sources and enrichment mechanisms of Li-rich geothermal springs in the Mediterranean–Himalayan belt: Modelling from Li isotope and hydrochemistry. *Geol. J.* **2025**, *60*, 2019–2032. https://doi.org/10.1002/gj.5134
82. Wang, C.; Zheng, M.; Zhang, X.; et al. O, H and Sr isotope evidence for origin and mixing processes of the Gudui geothermal system, Himalayas, China. *Geosci. Front.* **2020**, *11*, 1175–1187. https://doi.org/10.1016/j.gsf.2019.09.013
83. Yuan, X.; Zhang, Y.; Huang, J.; et al. Hydrochemistry and multi-Isotopes for interpreting formation mechanisms of different-type geothermal waters in the Cuona-Woka Rift, Southern Tibetan plateau. *Geosci. Front.* **2025**, *16*, 102170. https://doi.org/10.1016/j.gsf.2025.102170
84. Shi, Z.; Tan, H.; Cong, P.; et al. Speciation distribution and phase partition laws of rare alkali metals in geothermal Sinter deposits in Southern Tibet: Implications for the cesium mineralisation in the geothermal system. *Chem. Geol.* **2025**, *692*, 122975. https://doi.org/10.1016/j.chemgeo.2025.122975
85. Qiang, K.; Tan, H.; Shi, Z.; et al. Study on the genetic relationship between siliceous rocks and surrounding cesium-rich siliceous Sinter in the Gudui Area of Xizang. *Geol. Explor.* **2025**. https://doi.org/10.12134/j.dzykt.2025.06.023
86. Zhou, Y.; Fu, W.; Yang, Z.; et al. Geochemical characteristics of Mesozoic chert from southern Tibet and its petrogenic implications. *Acta Petrol. Sin.* **2008**, *24*, 600–608. https://doi.org/10.18654/10000569/2008.03.600608.
87. Tong, W.; Zhang, M.T.; Zhang, Z.F.; et al. *Geothermals Beneath Xizang(Tibetan) Plateau*; Beijing Science and Technology Press: Beijing, China, 1981.
88. Pan, S.; Zhao, P.; Guan, H.; et al. Mechanisms of lithium and cesium enrichment in the semi-Dazi geothermal field, Qinghai-Xizang plateau: Insights from H–O–Li–Sr isotopes. *Geotherm. Energy* **2025**, *13*, 22. https://doi.org/10.1186/s40517-025-00348-3
89. Millot, R.; Hegan, A.; Négrel, P. Geothermal waters from the Taupo Volcanic zone, New Zealand: Li, B and Sr isotopes characterization. *Appl. Geochem.* **2012**, *27*, 677–688. https://doi.org/10.1016/j.apgeochem.2011.12.015
90. Li, T.; Liu, J.-Q.; Wang, X.-H.; et al. Geochemical characteristics and genesis of gases from Tianchi Volcanic Springs. Changbai Mountains. Jilin, China. *Bull. Mineral. Petrol. Geochem.* **2015**, *34*, 1192–1202. https://doi.org/10.3969/j.issn.l007-2802.2015.06.011
91. McDonough, W. F.; Sun, S.-S. The composition of the Earth. *Chem. Geol.* **1995**, *120*, 223–253. https://doi.org/10.1016/00092541(94)001404
92. Hu, F.; Liu, X.; He, S.; et al. Cesium–rubidium mineralization in Himalayan leucogranites. *Sci. China Earth Sci.* **2023**, *66*, 2827–2852. https://doi.org/10.1007/s11430-022-1159-3
93. Li, J.; Song, X. Tearing of Indian mantle lithosphere from high-resolution seismic images and its implications for lithosphere coupling in Southern Tibet. *Proc. Natl. Acad. Sci. USA* **2018**, *115*, 8296–8300. https://doi.org/10.1073/pnas.1717258115
94. Karakas, O.; Dufek, J.; Mangan, M.T.; et al. Thermal and petrologic constraints on lower crustal melt accumulation under the Salton sea geothermal field. *Earth Planet. Sci. Lett.* **2017**, *467*, 10–17. https://doi.org/10.1016/j.epsl.2017.02.027
95. Kühn, C.; Brasse, H.; Schwarz, G. Three-dimensional electrical resistivity image of the volcanic arc in northern Chile—an appraisal of early magnetotelluric data. *Pure Appl. Geophys.* **2018**, 175, 2153–2165.
96. Wu, F.Y.; Liu, X.C.; Liu, Z.C.; et al. Highly fractionated Himalayan leucogranites and associated rare-metal mineralization. *Lithos* **2020**, *352–353*, 105319. https://doi.org/10.1016/j.lithos.2019.105319
97. Cao, H.-W.; Pei, Q.-M.; Santosh, M.; et al. Himalayan leucogranites: A review of geochemical and isotopic characteristics, timing of formation, genesis, and rare metal mineralization. *Earth-Sci. Rev.* **2022**, *234*, 104229. https://doi.org/10.1016/j.earscirev.2022.104229
98. Tsumura, A.; Yamasaki, S. Background levels of trace elements in rain and river waters in Japan. *R*adioisotopes **1998**, *47*, 46–55. https://doi.org/10.3769/radioisotopes.47.46
99. Klemm, L.M.; Pettke, T.; Heinrich, C.A. Fluid and source magma evolution of the Questa porphyry Mo deposit, New Mexico, USA. *Miner. Depos.* **2008**, *43*, 533–552. https://doi.org/10.1007/s00126-008-0181-7
100. Yuan, Y.; Chen, B.; Shang, L.; et al. Lithium enrichment of magmatic–hydrothermal fluids in albite–spodumene pegmatite from Lijiagou, Eastern Tibetan Plateau: Evidence from fluid inclusions. *Ore Geol. Rev.* **2023**, *162*, 105685. https://doi.org/10.1016/j.oregeorev.2023.105685
101. Tan, H.; Zhang, Y.; Zhang, W.; et al. Understanding the circulation of geothermal waters in the Tibetan Plateau using oxygen and hydrogen stable isotopes *Appl. Geochem.* **2014**, *51*, 23–32. https://doi.org/10.1016/j.apgeochem.2014.09.006
102. Yang, L.; Wang, J.-M.; Liu, X.-C.; et al. Petrogenetic link between leucogranite and spodumene pegmatite in Lhozhag, eastern Himalaya: Constraints from U–(Th)–Pb geochronology and Li–Nd–Hf isotopes. *Lithos* **2024**, *470–471*, 107530. https://doi.org/10.1016/j.lithos.2024.107530
103. Zhao, H.; Chen, B.; Huang, C.; et al. Geochemical and Sr–Nd–Li isotopic constraints on the genesis of the Jiajika Li-rich pegmatites,

eastern Tibetan Plateau: Implications for Li mineralization. *Contrib. Mineral. Petrol.* **2021**, *177*, 4. https://doi.org/10.1007/S00410-021-01869-3

104. Gao, P.; Zheng, Y.-F.; Mayne, M.J.; et al. Miocene high-temperature leucogranite magmatism in the Himalayan orogen. *GSA Bull.* **2020**, *133*, 679–690. https://doi.org/10.1130/B35691.1
105. Xie, L.; Tao, X.; Wang, R.; et al. Highly fractionated leucogranites in the eastern Himalayan Cuonadong dome and related magmatic Be–Nb–Ta and hydrothermal Be–W–Sn mineralization. *Lithos* **2020**, *354–355*, 105286. https://doi.org/10.1016/j.lithos.2019.105286
106. Fan, J.-J.; Tang, G.-J.; Wei, G.-J.; et al. Lithium isotope fractionation during fluid exsolution: Implications for Li mineralization of the Bailongshan pegmatites in the West Kunlun, NW Tibet. *Lithos* **2020**, *352*, 105236. https://doi.org/10.1016/j.lithos.2019.105236
107. Troch, J.; Huber, C.; Bachmann, O. The physical and chemical evolution of magmatic fluids in near-solidus silicic magma reservoirs: Implications for the formation of pegmatites. *Am. Mineral.* **2022**, *107*, 190–205. https://doi.org/10.2138/am-2022-7997
108. Thomas, R.; Davidson, P.; Badanina, E. A melt and fluid inclusion assemblages in beryl from pegmatite in the Orlovka amazonite granite, East Transbaikalia, Russia: Implications for pegmatite-forming melt systems. *Miner. Petrol.* **2009**, *96*, 129–140. https://doi.org/10.1007/s00710-009-0053-6
109. Wang, G.; Liu, Y.; Zhu, X.; et al. The status and development trend of geothermal resources in China. *Earth Sci. Front.* **2020**, *27*, 191–201. https://doi.org/10.13745/j.esf.sf.2020.1.1
110. Casey, W.H.; Sposito, G. On the temperature dependence of mineral dissolution rates. *Geochim. Cosmochim. Acta* **1992**, *56*, 3825–3830. https://doi.org/10.1016/0016-7037(92)90173-G
111. Walter, M.R.; Desmarais, D.; Farmer, J.D.; et al. Lithofacies and biofacies of mid-Paleozoic thermal spring deposits in the Drummond Basin, Queensland, Australia. *PALAIOS* **1996**, *11*, 497–518. https://doi.org/10.2307/3515199
112. De Filippis, L.; Faccenna, C.; Billi, A.; et al. Plateau versus Fissure ridge travertines from Quaternary geothermal springs of Italy and Turkey: Interactions and feedbacks between fluid discharge, paleoclimate, and tectonics. *Earth-Sci. Rev.* **2013**, *123*, 35–52. https://doi.org/10.1016/j.earscirev.2013.04.001
113. Djokic, T.; Bolhar, R.; Brengman, L. A.; et al. Trace elements (REE + Y) reveal marine, subaerial, and hydrothermal controls on an early Archean habitat for life: The 3.48 Ga volcanic-caldera system of the dresser formation, Pilbara Craton. *Chem. Geol.* **2024**, *644*, 121865. https://doi.org/10.1016/j.chemgeo.2023.121865
114. McKenzie, E.J.; Brown, K.L.; Cady, S.L.; et al. Trace metal chemistry and silicification of microorganisms in geothermal Sinter, Taupo Volcanic Zone, New Zealand. *Geothermics* **2001**, *30*, 483–502. https://doi.org/10.1016/S0375-6505(01)00006-9
115. Hartman, I.E.; Tan, H.; Shi, D.; et al. Elemental distribution and partitioning law between the geothermal water and associated deposits for a typical geothermal system with large-scale siliceous sinter deposits in the Tibet. *Geochem. Int.* **2021**, *59*, 1258–1273. https://doi.org/10.1134/S0016702921130032
116. Baek, W.; Avramov, P.V.; Kim, Y. Nuclear magnetic resonance and theoretical simulation study on Cs ion Co-adsorbed with other alkali cations on illite. *Appl. Surf. Sci.* **2019**, *489*, 766–775. https://doi.org/10.1016/j.apsusc.2019.06.039
117. Boudreau, A.E.; Lynne, B.Y. The growth of siliceous sinter deposits around high-temperature eruptive hot springs. *J. Volcanol. Geotherm. Res.* **2012**, *247–248*, 1–8. https://doi.org/10.1016/j.jvolgeores.2012.07.008
118. Zhou, B.; Ren, E.; Sherriff, B.L.; et al. Multinuclear NMR study of Cs-bearing geyserites of the Targejia hot spring cesium deposit in Tibet. *Am. Mineral.* **2013**, *98*, 907–913. https://doi.org/10.2138/am.2013.4321
119. Liu, R.; Liu, F.; Hu, C.; et al. Simultaneous removal of Cd(II) and Sb(V) by Fe–Mn binary oxide: Positive effects of Cd(II) on Sb(V) adsorption. *J. Hazard. Mater.* **2015**, *300*, 847–854. https://doi.org/10.1016/j.jhazmat.2015.08.010
120. Yang, K.; Liu, Y.; Li, Y.; et al. Applications and characteristics of Fe–Mn binary oxides for Sb(V) removal in textile wastewater: Selective adsorption and the fixed-bed column study. *Chemosphere* **2019**, *232*, 254–263. https://doi.org/10.1016/j.chemosphere.2019.05.174
121. Campbell, K.A.; Guido, D.M.; Gautret, P.; et al. Geyserite in hot-spring siliceous sinter: Window on Earth's hottest terrestrial (Paleo)Environment and its extreme life. *Earth-Sci. Rev.* **2015**, *148*, 44–64. https://doi.org/10.1016/j.earscirev.2015.05.003
122. Dobson, P.; Araya, N.; Brounce, M.; et al. *Characterizing the Geothermal Lithium Resource at the Salton Sea*; Lawrence Berkeley National Laboratory (LBNL): Berkeley, CA, USA, 2023. https://www.osti.gov/biblio/2222403 (accessed on 3 November 2024)
123. Gao, L.; Ma, G.; Zheng, Y.; et al. Research trends on separation and extraction of rare alkali metal from salt lake brine: Rubidium and cesium. *Solvent Extr. Ion Exch.* **2020**, *38*, 753–776. https://doi.org/10.1080/07366299.2020.1802820
124. Bolinger, M.; Millstein, D.; Gorman, W.; et al. Mind the gap: Comparing the net value of geothermal, wind, solar, and solar+ storage in the western United States. *Renew. Energy* **2023**, *205*, 999–1009. https://doi.org/10.1016/j.renene.2023.01.087
125. Ricks, W.; Voller, K.; Galban, G.; et al. The role of flexible geothermal power in decarbonized electricity systems. *Nat. Energy* **2025**, *10*, 28–40. https://doi.org/10.1038/s41560-024-01635-5
126. Pan, S.-Y.; Gao, M.; Shah, K.J.; et al. Establishment of enhanced geothermal energy utilization plans: Barriers and strategies. *Renew. Energy* **2019**, *132*, 19–32. https://doi.org/10.1016/j.renene.2018.07.036
127. Tester, J.W.; Beckers, K.F.; Hawkins, A.J.; et al. The evolving role of geothermal energy for decarbonizing the United States *Energy Environ. Sci.* **2021**, *14*, 6211–6241. https://doi.org/10.1039/D1EE02043F
128. Vargas, C.A.; Caracciolo, L.; Ball, P.J. Geothermal energy as a means to decarbonize the energy mix of megacities *Commun. Earth Environ.* **2022**, *3*, 66. https://doi.org/10.1038/s43247-022-00385-8
129. Wei, W.; Ge, Z.; Geng, Y.; et al. Toward carbon neutrality: Uncovering constraints on critical minerals in the Chinese power system. *Fundam. Res.* **2022**, *2*, 367–377. https://doi.org/10.1016/j.fmre.2022.01.005
130. Shi, H.; Heng, J.; Duan, H.; et al. Critical mineral constraints pressure energy transition and trade toward the Paris Agreement climate goals. *Nat. Commun.* **2025**, *16*, 4496. https://doi.org/10.1038/s41467-025-4496-4
131. Mousavinezhad, S.; Nili, S.; Fahimi, A.; et al. Environmental impact assessment of direct lithium extraction from brine resources: Global warming potential, land use, water consumption, and charting sustainable scenarios. *Resour. Conserv. Recycl.* **2024**, *205*, 107583. https://doi.org/10.1016/j.resconrec.2024.107583
132. Zhu, Y.; Hu, Y.; Zhu, Y. Can China's energy policies achieve the "dual carbon" goal? A multi-dimensional analysis based on policy text tools. *Environ. Dev. Sustain.* **2024**, *26*, 1–40. https://doi.org/10.1007/s10668-024-04637-3